Published for SISSA by Springer
Received: October 22, 2022
Accepted: December 1, 2022
Published: December 13, 2022

Gravity as a portal to reheating, leptogenesis and dark matter

Basabendu Barman,[a,b] **Simon Cléry,**[c] **Raymond T. Co,**[d] **Yann Mambrini**[c] **and Keith A. Olive**[d]

[a] *Centro de Investigaciones, Universidad Antonio Nariño, Carrera 3 este # 47A-15, Bogotá, Colombia*
[b] *Institute of Theoretical Physics, Faculty of Physics, University of Warsaw, ul. Pasteura 5, 02-093 Warsaw, Poland*
[c] *Université Paris-Saclay, CNRS/IN2P3, IJCLab, 91405 Orsay, France*
[d] *William I. Fine Theoretical Physics Institute, School of Physics and Astronomy, University of Minnesota, Minneapolis, MN 55455, U.S.A.*

E-mail: basabendu88barman@gmail.com, simon.clery@ijclab.in2p3.fr, rco@umn.edu, yann.mambrini@ijclab.in2p3.fr, olive@physics.umn.edu

Abstract: We show that a minimal scenario, utilizing only the graviton as an intermediate messenger between the inflaton, the dark sector and the Standard Model (SM), is able to generate *simultaneously* the observed relic density of dark matter (DM), the baryon asymmetry through leptogenesis, as well as a sufficiently hot thermal bath after inflation. We assume an inflaton potential of the form $V(\phi) \propto \phi^k$ about the minimum at the end of inflation. The possibility of reheating via minimal gravitational interactions has been excluded by constraints on dark radiation for excessive gravitational waves produced from inflation. We thus extend the minimal model in several ways: i) we consider non-minimal gravitational couplings — this points to the parameter range of DM masses $M_{N_1} \simeq 2$–$10\,\text{PeV}$, and right-handed neutrino masses $M_{N_2} \simeq (5\text{–}20) \times 10^{11}\,\text{GeV}$, and $T_{\rm RH} \lesssim 3 \times 10^5\,\text{GeV}$ (for $k \leq 20$); ii) we propose an explanation for the PeV excess observed by IceCube when the DM has a direct but small Yukawa coupling to the SM; and iii) we also propose a novel scenario, where the gravitational production of DM is a two-step process, first through the production of two scalars, which then decay to fermionic DM final states. In this case, the absence of a helicity suppression enhances the production of DM and baryon asymmetry, and allows a great range for the parameters including a dark matter mass below an MeV where dark matter warmness can be observable by cosmic 21-cm lines, even when gravitational interactions are responsible for reheating. We also show that detectable primordial gravitational wave signals provide the opportunity to probe this scenario for $T_{\rm RH} \lesssim 5 \times 10^6\,\text{GeV}$ in future experiments, such as BBO, DECIGO, CE and ET.

Keywords: Early Universe Particle Physics, Particle Nature of Dark Matter, Baryo-and Leptogenesis, Models for Dark Matter

ArXiv ePrint: 2210.05716

https://doi.org/10.1007/JHEP12(2022)072

JHEP12(2022)072

Contents

1 Introduction

Since the first calculation of the mass of the Milky Way by Henry Poincaré in 1906 [1], and the conclusion that the *"dark matter is present in much greater amount than luminous matter"* by Fritz Zwicky in 1933 [2], the virial method has been used frequently to compute the amount of dark matter (DM) in the Universe. The presence of dark matter is generally deduced from its gravitational effects. The precise abundance of DM is obtained from observations of the anisotropy spectrum of the cosmological microwave background (CMB) [3]. Initially, a neutrino, or more generally a heavy neutral lepton was thought to be an ideal dark matter candidate [4]. This candidate was assumed to interact weakly with the Standard Model (SM) and required a GeV scale mass to satisfy relic abundance constraints [5, 6]. Generalizations of the heavy neutrino DM candidate are referred to as WIMPs (weakly interacting massive particles). Perhaps the best studied WIMP is the lightest supersymmetric particle in supersymmetric extensions of the SM [7]. Other well studied candidates include those generated by a Higgs-portal [8–18] or a Z-portal [19, 20]. However, these minimal constructions are now heavily constrained (see, for example, refs. [21, 22] for reviews), and even extensions to Z'-portal [23–27] are in tension with the electroweak nature of dark matter.

The WIMP relic density is often determined by thermal freeze-out. WIMPs are assumed to be in thermal equilibrium at temperatures higher than the mass, and the relic density is determined by the equilibrium density when DM annihilations can no longer keep up

JHEP12(2022)072

with the expansion rate of the Universe. It is also possible that particles with interactions much weaker than electroweak interactions and are never fully in equilibrium, but are nonetheless produced in the thermal bath after inflation. An example of such a candidate is the gravitino [7, 28–30]. More generally, these Feebly Interacting Massive Particles (FIMPs) have been proposed [31–33] as an alternative to WIMPs (see [34] for a recent review). In this framework, the DM candidate is never thermalized due its extremely weak coupling to the SM, so weak that they evade the current accelerator constraints.

In the early Universe, FIMPs can be produced from either the decay or annihilation of states in the visible sector. When the SM temperature becomes smaller than the typical mass scale of the interaction (i.e. the maximum of the DM and the mediator mass), the generation process becomes suppressed, leaving a constant comoving DM number density. Such a scenario is often referred as the freeze-in mechanism [32]. In contrast to the "WIMP-miracle" which produces the observed relic density with near weak-scale couplings and masses, a "FIMP-miracle" occurs when one considers renormalizable couplings of order $\sim \mathcal{O}(10^{-11})$ independent of the mass of the DM. If a priori such couplings seem unatural, UV versions of the freeze-in mechanism may invoke *effective* couplings, suppressed by a large mass scale above the temperature of the thermal bath. This can be achieved via non-renormalizable operators [35], suppressed by a high mass scale, e.g., in models where the mediators between the visible sector and the dark sectors are very massive. This is the case in unified theories like SO(10) with a heavy Z' gauge boson [33, 36, 37], moduli fields [38], high scale SUSY [39–43] or heavy spin-2 constructions [44]. In other examples, freeze-in of DM may proceed via loops [45, 46] or 4-body final states [47]. All of these scenarios are particularly interesting, as the DM yield is sensitive to the highest temperature $T_{\rm max}$ reached by the SM plasma [48–53], controlled by the dynamics of the inflaton decay.

Even feebler interactions are possible when the only effective coupling at the UV scale is gravity. Indeed, the minimal irreducible interaction that should exist between DM and the Standard Model (SM) is mediated by graviton exchange [44, 54–71] which can lead to the observed amount of DM through the scattering of the particles in the thermal bath or directly through the gravitational transfer of the energy stored in the inflaton condensate, as already been discussed in detail refs. [65–69].

DM requires an extension to the SM, but it is not the only reason why an extension is necessary. As is well known, the visible or baryonic matter content of the Universe is asymmetric. One interesting mechanism to produce the baryon asymmetry of the Universe (BAU) via the lepton sector physics is known as leptogenesis [72], where, instead of creating a baryon asymmetry directly, a lepton asymmetry is generated first and subsequently gets converted into baryon asymmetry by the $(B + L)$-violating electroweak sphaleron transitions [73]. In thermal leptogenesis [74–77], the decaying particles, typically right-handed neutrinos (RHNs), are produced thermally from the SM bath. However, the lower bound on the RHN mass in such scenarios (known as the Davidson-Ibarra bound), leads to a lower bound on the reheating temperature $T_{\rm RH} \gtrsim 10^{10}\,\text{GeV}$ [78] so that the RHNs can be produced from the thermal bath. One simpler alternative is the non-thermal production of RHNs [79–83] originating from the decay of inflaton. This interaction is necessarily model dependent as it depends on the Yukawa interaction between the inflaton and the RHNs.

JHEP12(2022)072

In addition to providing the DM abundance, gravitational interactions can also be the source of baryogenesis. As shown in [84], it is possible to have a model-independent theory of non-thermal production of RHNs from inflation, once the inflaton potential is specified.[1] The abundance of RHNs is calculated in the same manner as the dark matter abundance and can lead to observed BAU from the out-of-equilibrium CP violating decay of the RHNs, produced during the reheating epoch.

As noted above, the DM and RHNs may be produced through gravitational interactions emanating from the thermal bath or directly from the inflaton condensate. It has also been argued that the thermal bath itself may be generated from gravitational interactions [68, 84, 86]. However, reheating the Universe from graviton exchange processes alone requires a steep inflaton potential during reheating, resulting in a low reheating temperature and a massive enhancement of tensor modes after inflation. Hence, the minimal scenario of gravitational reheating is excluded by an excessive generation of dark radiation in the form of gravitational waves (GWs) during BBN, as already noted in [87]. This limitation of minimal gravitational reheating is one motivation to introduce, as a natural generalization, non-minimal couplings of fields with gravity.

Motivated by these arguments, we derive a simultaneous solution for the DM abundance, the baryon asymmetry, and the origin of the thermal bath from purely gravitational interactions. In this sense, our scenario can be considered as the most minimal possible, since we do not introduce any new interactions for any process beyond the SM, except for gravity. The only new fields required are the dark matter candidate and the RHNs (which are anyway needed for the generation of neutrino masses). Our only model dependence comes from the choice of the particular inflaton potential. However we are mostly sensitive to the shape of the potential about the minimum after inflation. To be definite, we adopt the class of inflationary models called T-models [88]. But, as will be shown, even this dependence proves to be weak when it comes to combining the constraints of reheating, baryogenesis, and the dark matter relic density. We further show that the present framework can give rise to a detectable inflationary GW background, that in turn excludes the minimal gravitational reheating scenario which leads to an excess of the present-day GW energy density, in conflict with the BBN prediction. However, a large part of the parameter space still remain within the reach of several futuristic GW detection facilities.

The paper is organized as follows. After presenting our framework in section 2, we review the gravitational production from inflaton scattering and the thermal bath in section 3, where we also discuss the effect of non-minimal gravitational interactions. We derive the set of parameters (dark matter mass, RHN mass, and reheating temperature, $T_{\rm RH}$, which simultaneously provide the correct relic density and BAU in section 4. If the dark matter is not absolutely stable, we are able to propose an explanation for the PeV events observed at IceCube in the case of a long-lived candidate. Finally, we propose a novel scenario where the gravitational production is a two-step process passing through a scalar singlet which couples with the RHN sector in section 5, before concluding in section 6.

[1] The simultaneous generation of gravitational DM and the baryon asymmetry was also discussed in [85]. Our results differ, as their choices of parameters are in conflict with the tensor-to-scalar ratio bound from Planck.

JHEP12(2022)072

2 The framework

If the metric is expanded around Minkowski space-time: $g_{\mu\nu} \simeq \eta_{\mu\nu} + \frac{2h_{\mu\nu}}{M_P}$, then the gravitational interactions are described by the Lagrangian [89, 90]

$$\sqrt{-g}\,\mathcal{L}_{\rm int} = -\frac{1}{M_P}\,h_{\mu\nu}\left(T^{\mu\nu}_{\rm SM} + T^{\mu\nu}_{\phi} + T^{\mu\nu}_{X}\right), \tag{2.1}$$

where ϕ is the inflaton and X is a particle which does not belong to the SM.[2] In the present context we consider X to be a spin 1/2 Majorana fermion which can be associated with the dark matter or a right-handed neutrino. The graviton propagator for momentum p is

$$\Pi^{\mu\nu\rho\sigma}(p) = \frac{\eta^{\rho\nu}\eta^{\sigma\mu} + \eta^{\rho\mu}\eta^{\sigma\nu} - \eta^{\rho\sigma}\eta^{\mu\nu}}{2p^2}\,. \tag{2.2}$$

The form of the stress-energy tensor $T^{\mu\nu}_i$ depends on the spin of the field and, for Majorana spin-1/2 fermions, takes the form

$$T^{\mu\nu}_{1/2} = \frac{i}{8}\left[\bar{\chi}\gamma^{\mu}\overleftrightarrow{\partial^{\nu}}\chi + \bar{\chi}\gamma^{\nu}\overleftrightarrow{\partial^{\mu}}\chi\right] - g^{\mu\nu}\left[\frac{i}{4}\bar{\chi}\gamma^{\alpha}\overleftrightarrow{\partial_{\alpha}}\chi - \frac{m_{\chi}}{2}\,\overline{\chi^{c}}\chi\right], \tag{2.3}$$

whereas for a scalar φ,

$$T^{\mu\nu}_0 = \partial^{\mu}\varphi\partial^{\nu}\varphi - g^{\mu\nu}\left[\frac{1}{2}\partial^{\alpha}\varphi\,\partial_{\alpha}\varphi - V(\varphi)\right]. \tag{2.4}$$

There are of course many possible scalar potentials $V(\phi)$ which can account for inflation. However, the calculations relevant in this paper are largely independent of the potential during inflation and depend only on the shape of the potential about the minimum. Without loss of generality, we will assume that $V(\phi)$ is among the class of α-attractor T-models [88]

$$V(\phi) = \lambda M_P^4\left|\sqrt{6}\tanh\left(\frac{\phi}{\sqrt{6}M_P}\right)\right|^{k}, \tag{2.5}$$

which can be expanded about the origin[3]

$$V(\phi) = \lambda\frac{\phi^k}{M_P^{k-4}}\,; \quad \phi \ll M_P\,. \tag{2.6}$$

In this class of models, inflation occurs at large field values ($\phi > M_P$), and after the period of exponential expansion, the inflaton begins to oscillate about the minimum and the process of reheating begins. The end of inflation may be defined when $\ddot{a} = 0$ where a is the cosmological scale factor. The inflaton field value at that time is given by [52, 91] as

$$\phi_{\rm end} \simeq \sqrt{\frac{3}{8}}M_P\ln\left[\frac{1}{2} + \frac{k}{3}\left(k + \sqrt{k^2+3}\right)\right]. \tag{2.7}$$

[2] $M_P = (8\pi G_N)^{-1/2} \simeq 2.4\times10^{18}$ GeV is the reduced Planck mass.

[3] Our discussion is general and not limited to T-models of inflation as the way we express the minimum of the potential is generic.

JHEP12(2022)072

It is easy to show that at the end of inflation, the condition $\ddot{a} = 0$ is equivalent to $\dot{\phi}^2_{\rm end} = V(\phi_{\rm end})$ and thus the inflaton energy density at $\phi_{\rm end}$ is $\rho_{\rm end} = \frac{3}{2}V(\phi_{\rm end})$. The overall scale of the potential parameterized by the coupling λ, can be determined from the amplitude of the CMB power spectrum A_S,

$$\lambda \simeq \frac{18\pi^2 A_S}{6^{k/2} N^2}, \tag{2.8}$$

where N is the number of e-folds measured from the end of inflation to the time when the pivot scale $k_* = 0.05\,{\rm Mpc}^{-1}$ exits the horizon. In our analysis, we use $\ln(10^{10} A_S) = 3.044$ [92] and set $N = 55$. This leads to an inflaton mass of $m_\phi \simeq 1.2 \times 10^{13}\,{\rm GeV}$ for $k = 2$. More generically, $m_\phi \simeq 1.2 \times 10^{13}$ is also the inflaton mass at the end of inflation for any larger k when the full potential in eq. (2.5) is used. While $N = 55$ is appropriate for reheating temperatures of order $10^{12}\,{\rm GeV}$, for lower reheating temperatures (between 10–$10^7\,{\rm GeV}$) $N =$ 45–50 [93]. However, we have checked that our results are very insensitive to the value of N.

In addition to the inflationary sector and the SM, neutrino masses and mixing require at least two (heavy) right-handed neutrino states for the seesaw mechanism [94–99]. One of these, if produced and remaining out-of-equilibrium until its decay, can produce a lepton asymmetry. In order to account for the dark matter in a most economic way, we assume three RHNs, N_i, where for now, the lightest of these, N_1 is decoupled from the other two and has a vanishing Yukawa coupling. Aside from the Yukawa couplings, the only couplings we consider between the SM, the RHNs, and the inflaton are gravitational of the form in eq. (2.1). Needless to say, such interactions are unavoidable, and must be taken into account in any extensions beyond the SM.

As a concrete example, we consider the renormalizable interaction Lagrangian between the Majorana RHNs and the SM

$$\mathcal{L} \supset -\frac{1}{2} M_{N_i} \overline{N_i^c} N_i - (y_N)_{ij}\, \overline{N}_i\, \widetilde{H}^\dagger\, L_j + \text{h.c.}\,. \tag{2.9}$$

Here H and L are the SM Higgs and lepton doublet respectively. Lepton number is clearly violated in this Lagrangian.[4] For now, we assume that $(y_N)_{1i} = 0$ for all i and that N_1 is stable. As a result, N_1 is a viable DM candidate. Later, we will relax this condition and consider a metastable DM candidate with $(y_N)_{1i} \neq 0$, allowing for N_1 to decay into neutrinos that could be observed at IceCube. The preservation of the lepton asymmetry will provide a limit on $(y_N)_{1i}/M_{N_1}$. The other two RHNs, namely $N_{2,3}$ are assumed to be heavier and they participate in leptogenesis.

We would like to remind the readers that there are three types of seesaw models, which differ by the properties of the exchanged heavy particles, e.g.,

(i) Type-I: SM gauge fermion singlets

(ii) Type-II: SM $\mathrm{SU}(2)_L$ scalar triplets

(iii) Type-III: SM $\mathrm{SU}(2)_L$ fermion triplets.

[4] We consider the RHNs to be mass diagonal.

JHEP12(2022)072

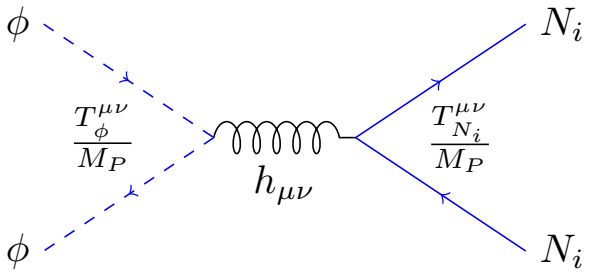

Figure 1. Feynman diagram for the production of RHN through the gravitational scattering of the inflaton condensate. A similar diagram also exists with Standard Model particles in the initial state.

In the present case we are considering the Type-I scenario, which is evident from the Lagrangian in eq. (2.9). The Type-I seesaw mechanism can indeed be realized with only two active right-handed neutrino [100–103]. In this context, only the normal ($m_1 < m_2 < m_3$) and inverted ($m_3 < m_2 < m_1$) hierarchies are relevant, where m_i are the light neutrino masses. With only two RHN playing a role in the seesaw mechanism, we expect $m_1 = 0$ or $m_3 = 0$, depending on the hierarchy. Indeed, due to the reduced rank of the mass matrices (a 3×2 Dirac matrix and a 2×2 Majorana matrix) one neutrino remains massless, while the others acquire their light mass through the usual seesaw suppression of the order $m_i \sim \frac{(y_N)^2_{ii}\langle H\rangle^2}{M_{N_i}}$.

We further assume the absence of any direct coupling between the inflaton ϕ and the RHNs, such that there is no perturbative decay of the inflaton into the RHN final state; in other words we do not attribute a lepton number to the inflaton. Thus, the *only* possible production of the RHNs is the 2-to-2 gravitational scattering of the inflatons and of the particles in the radiation bath. As we will show, these production channels dominate in different regions of the parameter space. In figure 1, we show the s-channel exchange of a graviton obtained from the Lagrangian in eq. (2.1) for the production of RHNs from the inflaton condensate, to which we can add a similar diagram for the production of SM fields during the reheating process. Despite the a priori Planck reduced interactions, we will show that this framework is perfectly capable of simultaneously explaining the dark matter relic abundance and the observed baryon asymmetry, while also reheating the Universe. The Planck suppression due to graviton exchange is indeed partially compensated by the energy available in the inflaton condensate at the end of inflation.

3 Gravitational production of RHNs

In this section, we compute the gravitational interactions and resulting abundances of the dark matter candidate, N_1 as well as the abundance of the RHN neutrino responsible for leptogenesis. We are particularly interested in the interactions of the type in figure 1 between the inflaton and the N_i. In addition, we are interested in the gravitational interactions between the inflaton and SM particles which make up the thermal bath. Furthermore, we will show that it is possible to produce the thermal bath assuming the absence of any inflaton decay mode leading to reheating. We will quantify how such interactions can give

JHEP12(2022)072

rise to reasonable relic density and baryon asymmetry. The DM candidate N_1 can be produced during reheating from inflaton scattering $\phi\phi \to N_1 N_1$ as well as from the thermal bath (mediated by a massless graviton in both cases). For $(y_N)_{1i} = 0$, N_1 couples only gravitationally, and the SM processes will not lead to its production. On the other hand, for the generation of the baryon asymmetry, we will cater to non-thermal leptogenesis, where the RHNs $N_{2,3}$ are too weakly coupled to reach thermal equilibrium. Hence they are predominantly produced only during reheating from gravitational inflaton scattering. To summarize, we consider the following production via graviton exchange

- $\phi\,\phi \to N_1\,N_1$, SM SM $\to N_1\,N_1$ for production of the DM candidate N_1.
- $\phi\,\phi \to N_{2,3}\,N_{2,3}$ for production of $N_{2,3}$ that will lead to non-thermal leptogenesis. (Contributions from SM SM $\to N_{2,3}\,N_{2,3}$ are negligibly small.)
- $\phi\phi \to$ SM SM for the reheating process.

In the following subsections we determine the production rate of DM and RHNs from the processes listed above.

3.1 Gravitational dark matter

We start by computing the DM number density via 2-to-2 scattering of the bath particles, mediated by graviton exchange. In this case the interaction rate is given by [44, 66, 68, 85]

$$R^T_{N_i} = \frac{1}{2} \times \beta_{1/2}\,\frac{T^8}{M_P^4}\,, \tag{3.1}$$

where we have $\beta_{1/2} = 11351\pi^3/10368000 \simeq 3.4\times10^{-2}$ [68], the explicit factor of $\frac{1}{2}$ accounting for the Majorana nature of N_i. The evolution of RHN number density n_{N_i} (with $i = 1, 2, 3$) is governed by the Boltzmann equation

$$\frac{dn_{N_i}}{dt} + 3\,H\,n_{N_i} = R^T_{N_i}\,, \tag{3.2}$$

where $H = \dot{a}/a$ is the Hubble parameter. Defining the comoving number density as $Y_{N_i} = n_{N_i}\,a^3$ we can re-cast the Boltzmann equation as

$$\frac{dY^T_{N_i}}{da} = \frac{a^2}{H}\,R^T_{N_i}\,, \tag{3.3}$$

where $i = 1$ for DM production, and the superscript T refer to the thermal source of production. In order to properly capture the evolution of the inflaton and radiation energy density (and hence temperature) we solve the following set of coupled equations

$$\begin{aligned}
&\frac{d\rho_\phi}{dt} + 3H\,(1+w_\phi)\,\rho_\phi = -(1+w_\phi)\,\Gamma_\phi\,\rho_\phi\,,\\
&\frac{d\rho_R}{dt} + 4H\,\rho_R = +(1+w_\phi)\,\Gamma_\phi\,\rho_\phi\,,
\end{aligned} \tag{3.4}$$

where $w_\phi \equiv \frac{p_\phi}{\rho_\phi} = \frac{k-2}{k+2}$ [52] is the general equation of state parameter, ρ_ϕ the inflaton energy density, $\rho_R = \frac{\pi^2 g_*}{30}\,T^4 \equiv c_*\,T^4$, and g_* is the effective number of degrees of freedom for the

JHEP12(2022)072

thermal plasma at the temperature T. We recall that in our framework the potential $V(\phi)$ is proportional to ϕ^k [see, eq. (2.6)].

During reheating, the total energy density is dominated by the inflaton and we can approximate the Hubble parameter by $H^2 \simeq \rho_\phi/3\,M_P^2$. In this case, it is possible to analytically solve eq. (3.4) and obtain

$$\rho_\phi(a) = \rho_{\rm end}\left(\frac{a_{\rm end}}{a}\right)^{\frac{6k}{k+2}}\,. \tag{3.5}$$

Recall that we are assuming that the radiation bath is produced *gravitationally* through inflaton scattering; namely, we do not rely on a specific decay channel $\phi \to$ SM particles for reheating. In this case, due to helicity conservation, the production of SM fermions from inflaton scattering is strongly suppressed by the mass of the fermions, whereas massless vectors are not produced because of the antisymmetry of $F_{\mu\nu}$. However, scattering into scalars, especially Higgs scalars, is always allowed and dominates the production rate. In [52], the inflaton dissipation rate was parameterized as $\Gamma_\phi \propto \rho_\phi^l$. For a quartic interaction with constant coupling, $l = (3/k) - (1/2)$. However, for the effective gravitational coupling between the inflaton and SM Higgs, the coupling is proportional to $m_\phi^2 \propto \rho_\phi^{(1-2/k)}$. This leads to $l = (3/2) - (1/k)$. More accurately, expanding the potential energy in terms of the Fourier modes [52, 68, 70, 84, 104, 105]

$$V(\phi) = V(\phi_0)\sum_{n=-\infty}^{\infty}\mathcal{P}_n^k e^{-in\omega t} = \rho_\phi\sum_{n=-\infty}^{\infty}\mathcal{P}_n^k e^{-in\omega t}\,, \tag{3.6}$$

the production rate of radiation is given by [68, 69, 84]

$$(1+w_\phi)\,\Gamma_\phi\,\rho_\phi = R_H^{\phi^k} \simeq \frac{N_h\rho_\phi^2}{16\pi M_P^4}\sum_{n=1}^{\infty}2n\omega|\mathcal{P}_{2n}^k|^2 = \alpha_k M_P^5\left(\frac{\rho_\phi}{M_P^4}\right)^{\frac{5k-2}{2k}}\,, \tag{3.7}$$

where $N_h = 4$ is the number of internal degrees of freedom for one complex Higgs doublet and we have neglected the Higgs bosons mass. The frequency of oscillations of ϕ is given by [52]

$$\omega = m_\phi\sqrt{\frac{\pi k}{2(k-1)}}\frac{\Gamma(\frac{1}{2}+\frac{1}{k})}{\Gamma(\frac{1}{k})}\,, \tag{3.8}$$

with $m_\phi^2 = \frac{\partial^2 V(\phi)}{\partial\phi^2}$ being the inflaton mass squared. The definition of α_k follows the analysis in [84], with the values given in table 1. For $l = (3/2) - (1/k)$ the results of [52] yields for the evolution of the radiation density

$$\rho_R(a) = \rho_{\rm RH}\left(\frac{a_{\rm RH}}{a}\right)^4\left[\frac{1-(a_{\rm end}/a)^{\frac{8k-14}{k+2}}}{1-(a_{\rm end}/a_{\rm RH})^{\frac{8k-14}{k+2}}}\right]\,, \tag{3.9}$$

which can be obtained by combining eqs. (3.4), (3.5) and (3.7). The evolution in eq. (3.9) is valid when $a_{\rm end} \ll a \ll a_{\rm RH}$ where $a_{\rm end}$ marks the end of inflation (or the onset of reheating), while $a_{\rm RH}$ indicates the end of reheating defined as $\rho_\phi(a_{\rm RH}) = \rho_R(a_{\rm RH}) = \rho_{\rm RH}$. To obtain eq. (3.5), we have supposed $H \gg \Gamma_\phi$, which is valid for all a because $\Gamma_\phi < H$ at

JHEP12(2022)072

k	α_k	α_k^ξ
6	0.000193	$\alpha_k + 0.00766\,\xi_h^2$
8	0.000528	$\alpha_k + 0.0205\,\xi_h^2$
10	0.000966	$\alpha_k + 0.0367\,\xi_h^2$
12	0.00144	$\alpha_k + 0.0537\,\xi_h^2$
14	0.00192	$\alpha_k + 0.0702\,\xi_h^2$
16	0.00239	$\alpha_k + 0.0855\,\xi_h^2$
18	0.00282	$\alpha_k + 0.0995\,\xi_h^2$
20	0.00322	$\alpha_k + 0.112\,\xi_h^2$

Table 1. Relevant coefficients for the gravitational reheating [cf. eq. (3.7) and eq. (3.50)].

the end of inflation and Γ_ϕ decreases faster than H for all $k \geq 2$. As a result, we note that gravitational reheating is only possible for $\frac{6k}{k+2} > 4$ [cf. eq. (3.5)], i.e., when ρ_ϕ redshifts faster than ρ_R. This limits our parameter space to $k > 4$. It is also important to ensure that a sufficiently large reheating temperature is attained to allow big bang nucleosynthesis to occur at $T \sim 1\,\text{MeV}$ as we will discuss in more detail in section 3.3.

Using eqs. (3.1) and (3.9) and relating T^8 to ρ_R^2, we obtain the thermal rate of DM production

$$R_{N_i}^T = \frac{1}{2} \times \beta_{1/2}\, \frac{\rho_{\rm RH}^2}{c_*^2\, M_P^4} \left(\frac{a_{\rm RH}}{a}\right)^8 \left[\frac{1-(a_{\rm end}/a)^{\frac{8k-14}{k+2}}}{1-(a_{\rm end}/a_{\rm RH})^{\frac{8k-14}{k+2}}}\right]^2 . \tag{3.10}$$

The DM number density at the end of reheating can then be computed by integrating eq. (3.3), leading to

$$\begin{aligned} n_{N_i}^T(a_{\rm RH}) = {} & \frac{\beta_{1/2}\,(k+2)\,\rho_{\rm RH}^{\frac{3}{2}}}{12\sqrt{3} M_P^3\, c_*^2} \left(\frac{1}{1-r^{\frac{14-8k}{k+2}}}\right)^2 \\ & \times \left[\frac{2(7-4k)^2}{(k+5)(k-1)(5k-2)}\, r^{\frac{10+2k}{k+2}} - \frac{9}{(k+5)} + \frac{18}{(5k-2)}\, r^{\frac{14-8k}{k+2}} - \frac{1}{(k-1)}\, r^{\frac{28-16k}{k+2}}\right], \end{aligned} \tag{3.11}$$

where $r = a_{\rm RH}/a_{\rm end}$. Since the gravitational reheating temperature is generally quite low as discussed in section 3.3, we can consider the limit $r \gg 1$ and the dominant term in the expression above is

$$n_{N_i}^T(a_{\rm RH}) \simeq \frac{\beta_{1/2}\,(k+2)\,\rho_{\rm RH}^{\frac{3}{2}}}{12\sqrt{3} M_P^3\, c_*^2}\, \frac{2(7-4k)^2}{(k+5)(k-1)(5k-2)}\, r^{\frac{10+2k}{k+2}} . \tag{3.12}$$

The contribution of gravitational scattering of the particles in the primordial plasma to the DM relic abundance can then be determined using [106]

$$\Omega_{N_1}^T\, h^2 = 1.6 \times 10^8\, \frac{g_0}{g_{\rm RH}}\, \frac{n_{N_1}^T(a_{\rm RH})}{T_{\rm RH}^3}\, \frac{M_{N_1}}{\text{GeV}} , \tag{3.13}$$

JHEP12(2022)072

which gives

$$\Omega_{N_1}^T h^2 \simeq 1.6\times 10^8 \times \frac{g_0\,\beta_{1/2}}{g_{\rm RH}} \times \frac{M_{N_1}}{\rm GeV}\,\frac{c_*^{-\frac{5}{6}-\frac{5}{3k}}\,(7-4k)^2\,(k+2)}{6\sqrt{3}\,(k+5)(k-1)(5k-2)}\left(\frac{T_{\rm RH}}{M_P}\right)^{\frac{5k-20}{3k}}\left(\frac{\rho_{\rm end}}{M_P^4}\right)^{\frac{k+5}{3k}}, \tag{3.14}$$

where $g_0 = g_*(T_0) = 43/11$ and $g_{\rm RH} = g_*(T_{\rm RH}) = 427/4$ are the number of relativistic degrees of freedom at present and at the end of reheating respectively. In (3.14), we have used eq. (3.5) evaluated at $a = a_{\rm RH}$ to relate r, $T_{\rm RH}$, and $\rho_{\rm end}$.

The DM candidate N_1 can also be produced directly from inflaton scattering. In fact, particle production directly from inflaton scattering can be much more efficient than gravitational thermal scattering when $T_{\rm RH}$ is low [68]. As we shall see in the next section, the same process is also involved in the production of the baryon asymmetry. For the production of N_1 through the scattering of the inflaton condensate, we consider the time dependent oscillations of a classical inflaton field $\phi(t)$.[5] The oscillating inflaton field with a time-dependent amplitude can be parametrized as

$$\phi(t) = \phi_0(t)\cdot\mathcal{Q}(t) = \phi_0(t)\sum_{n=-\infty}^{\infty}\mathcal{Q}_n e^{-in\omega t}, \tag{3.15}$$

where $\phi_0(t)$ is the time-dependent amplitude that includes the effects of redshift and $\mathcal{Q}(t)$ describes the periodicity of the oscillation. Furthermore, we assume a mass hierarchy $M_{N_{1,2,3}} < m_\phi$ such that the s-channel graviton mediated process (as shown in figure 1) is kinematically allowed. Note that, since N_1 is effectively decoupled from $N_{2,3}$, it does not necessarily need to be the lightest of the three. The production rate for N_i from inflaton scattering mediated by gravity is given[6] by [68]

$$R_{N_i}^{\phi^k} = \frac{\rho_\phi^2}{4\pi M_P^4}\,\frac{M_{N_i}^2}{m_\phi^2}\,\Sigma_{N_i}^k, \tag{3.16}$$

where

$$\Sigma_{N_i}^k = \sum_{n=1}^{+\infty}|\mathcal{P}_{2n}^k|^2\,\frac{m_\phi^2}{E_{2n}^2}\left[1-\frac{4\,M_{N_i}^2}{E_{2n}^2}\right]^{3/2}, \tag{3.17}$$

accounts for the sum over the Fourier modes of the inflaton potential, and $m_\phi^2 = \lambda\,k\,(k-1)\,\left(\rho_\phi/(\lambda\,M_P^4)\right)^{\frac{k-2}{k}}$. Here $E_n = n\omega$ is the energy of the n-th inflaton oscillation mode and

[5] As it has been pointed out in [107–109], for all potentials steeper than quadratic near the origin, the oscillating inflaton condensate may fragment due to self-resonance. The equation of state in that case approaches $w \to 1/3$ at sufficiently late times. If this occurs after $T = T_{\rm RH}$, then this effect is not important since the inflaton energy would already be subdominant. Furthermore, N is predominantly produced at $a_{\rm end}$ and so possible fragmentation at later times would not affect the calculation of the baryon asymmetry. Reheating may be affected; however, the exact time when w transitions 1/3 depends on k and requires dedicated lattice simulations. Self-resonance becomes less efficient for larger k as shown by the lattice results for k up to 6 [107–109], while most of our viable results are for $k > 6$. Performing such lattice simulations for larger k is beyond the scope of the present analysis.

[6] Note the difference of factor 2 with [68], comes from the Majorana nature of the RHNs.

JHEP12(2022)072

M_{N_i} is the mass of the produced RHN. Then, the number density of RHN is obtained by solving a Boltzmann equation analogous to that in eq. (3.3) as

$$\frac{dY_{N_i}^{\phi^k}}{da} = \frac{\sqrt{3}M_P}{\sqrt{\rho_{\rm RH}}}a^2\left(\frac{a}{a_{\rm RH}}\right)^{\frac{3k}{k+2}} R_{N_i}^{\phi^k}(a). \tag{3.18}$$

Integration of eq. (3.18), leads to the following expression for the RHN density [68, 84]

$$n_{N_i}^{\phi^k}(a_{\rm RH}) \simeq \frac{M_{N_1}^2\,\sqrt{3}\,(k+2)\,\rho_{\rm RH}^{\frac{1}{2}+\frac{2}{k}}}{24\,\pi\,k(k-1)\lambda^{\frac{2}{k}}\,M_P^{1+\frac{8}{k}}}\left(\frac{\rho_{\rm end}}{\rho_{\rm RH}}\right)^{\frac{1}{k}}\Sigma_{N_1}^k\,, \tag{3.19}$$

evaluated at the end of reheating. In order to obtain the DM relic abundance, one can again follow eq. (3.13), but now replacing $n_{N_1}^T(a_{\rm RH})$ with $n_{N_1}^{\phi}(a_{\rm RH})$, and obtain [68]

$$\begin{aligned}\frac{\Omega_{N_1}^{\phi^k}h^2}{0.12} = \frac{\Sigma_{N_1}^k}{2.4^{\frac{8}{k}}}\frac{k+2}{k(k-1)}\left(\frac{10^{-11}}{\lambda}\right)^{\frac{2}{k}}\left(\frac{10^{40}\,{\rm GeV}^4}{\rho_{\rm RH}}\right)^{\frac{1}{4}-\frac{1}{k}} \\ \times\left(\frac{\rho_{\rm end}}{10^{64}\,{\rm GeV}^4}\right)^{\frac{1}{k}}\left(\frac{M_{N_1}}{1.1\times10^{7+\frac{6}{k}}\,{\rm GeV}}\right)^3\,.\end{aligned} \tag{3.20}$$

The total DM relic abundance is a sum of the gravitational contribution from thermal bath ($\Omega_{N_1}^T\,h^2$) and from inflaton scattering ($\Omega_{N_1}^{\phi^k}\,h^2$).

3.2 Gravitational leptogenesis

Since N_1 is the stable DM candidate, in the present scenario the lighter of $N_{2,3}$ can undergo out-of-equilibrium decay to SM final states. We denote N_2 to be the lighter of these, and we must require that the mixing of N_1 and N_2 to be sufficiently small so as to prevent the decay of N_2 to N_1. For now, we take this coupling to be absent. The resulting CP asymmetry from the decay of N_2 is of the form [110–114]

$$\epsilon_{\Delta L} = \frac{\sum_\alpha[\Gamma(N_2\to l_\alpha+H)-\Gamma(N_2\to\bar{l}_\alpha+H^*)]}{\sum_\alpha[\Gamma(N_2\to l_\alpha+H)+\Gamma(N_2\to\bar{l}_\alpha+H^*)]}\,. \tag{3.21}$$

The resulting lepton asymmetry depends on the out-of-equilibrium abundance of N_2 as computed in the previous subsection. So long as $M_{N_2}\ll m_\phi$ and any kinematic suppression can be ignored, the number density of N_2 (at $a_{\rm RH}$) will be given by eq. (3.19) with the substitution $N_1\to N_2$. The CP asymmetry can be expressed as [43, 84, 113]

$$\epsilon_{\Delta L} \simeq \frac{3\delta_{\rm eff}}{16\,\pi}\,\frac{M_{N_2}\,m_{\nu\,,\rm max}}{v^2}\,, \tag{3.22}$$

where $\langle H\rangle\equiv v\approx 174\,{\rm GeV}$ is the SM Higgs doublet vacuum expectation value, $\delta_{\rm eff}$ is the effective CP violating phase in the neutrino mass matrix with $0\le\delta_{\rm eff}\le 1$, and, we take $m_{\nu,\rm max}=0.05\,{\rm eV}$ as the heaviest light neutrino mass.

Here we are interested in non-thermal leptogenesis [79, 81–83, 115–117]. The gravitationally produced N_2 should not be thermalized into the bath for the consistency of the calculation. To check this, we note that the thermalization rate $\Gamma_{\rm th}\simeq y_{N_2}^2T/8\pi$ decreases

JHEP12(2022)072

slower than the Hubble rate $H = \frac{\sqrt{\rho_\phi}}{\sqrt{3}M_P}$ based on eqs. (3.5) and (3.9). Thermalization is potentially dangerous until $T \simeq M_{N_2}$ when the N_2 out-of-equilibrium decay rate dominates over the thermalization rate. Using eq. (3.5), $a_{\rm end}/a \simeq T/T_{\rm max}$ based on eq. (3.9), and $y_{N_2} \simeq m_\nu M_{N_2}/v^2$, we find that $\Gamma_{\rm th}$ is always less than H at $T = M_{N_2}$ in the parameter space of interest.[7] Thus the resulting lepton asymmetry will not be suppressed by inverse decays.

The produced lepton asymmetry is eventually converted to baryon asymmetry via electroweak sphaleron processes leading to

$$Y_B = \frac{n_B}{s} = \frac{28}{79}\epsilon_{\Delta L}\,\frac{n^\phi_{N_2}(T_{\rm RH})}{s}\,, \tag{3.23}$$

where $n^\phi_{N_2}(T_{\rm RH})$ is the number density from eqs. (3.12) and (3.19) at the end of reheating and $s = 2\pi^2 g_{\rm RH} T^3_{\rm RH}/45$ is the entropy density. The final asymmetry then becomes

$$Y_B \simeq 3.5\times 10^{-4}\,\delta_{\rm eff}\left(\frac{m_{\nu,\rm max}}{0.05\,\text{eV}}\right)\left(\frac{M_{N_2}}{10^{13}\,\text{GeV}}\right)\left.\frac{n^\phi_{N_2}}{s}\right|_{T_{\rm RH}}\,, \tag{3.24}$$

while the observed value, as reported by Planck [3], is $Y_B^{\rm obs} \simeq 8.7\times 10^{-11}$.

We note that the lepton asymmetry is not washed out because the lepton-number violating process involving the Yukawa scattering and the electroweak sphaleron processes are never in equilibrium at the same time.

3.3 Gravitational reheating temperature

In section 3.1, we computed the energy density in radiation from purely gravitational process. However, to avoid conflict with the Big Bang nucleosynthesis (BBN), that requires the reheating temperature $T_{\rm RH} \gtrsim 1\,\text{MeV}$, one needs to consider[8] $w_\phi \gtrsim 0.65$ [84, 86], or $k = \frac{2\,(1+w_\phi)}{(1-w_\phi)} \gtrsim 9$. This lower bound comes from the fact that, for higher k, the inflaton energy density redshifts faster so the transition to radiation domination is achieved sooner, at a higher temperature.

The precise bound on $T_{\rm RH}$ is in fact more involved especially for $k \leq 8$ for the following reason. As noted below eq. (3.9), the inflaton-dominated era ends when ρ_ϕ redshifts below ρ_R as opposed to a complete transfer of the ϕ energy to radiation in conventional reheating by perturbative decays. Still, we define the reheating temperature $T_{\rm RH}$ by $\rho_\phi(T_{\rm RH}) = \rho_R(T_{\rm RH})$. The difference in the scale factor dependence between ρ_ϕ in eq. (3.5) and ρ_R in eq. (3.9) increases with k. In other words, for smaller k, the inflaton energy density does not redshift significantly more than radiation. Thus, $T_{\rm RH}$ for low k needs to be substantially higher than $T_{\rm BBN} \approx 1\,\text{MeV}$ so that the inflaton energy density does not excessively modify the expansion rate of the universe at BBN. We can recast the BBN bound on the extra energy density in the form of $\Delta N_\nu < 0.226$ [118] into a bound on $T_{\rm RH}$ as a function of k using the

[7] More precisely, $T/T_{\rm max} = a_{\rm max}/a = (a_{\rm max}/a_{\rm end})(a_{\rm end}/a) = ((6k-3)/(2k+4))^{((k+2)/(8k-14))}(a_{\rm end}/a) \approx 3^{1/8}(a_{\rm end}/a)$ for large k [68].

[8] This requirement of having large w_ϕ can be relaxed with non-minimal gravitational couplings as discussed in [69, 84].

JHEP12(2022)072

following expression

$$1 = \left.\frac{\rho_\phi}{\rho_R}\right|_{T_{\rm RH}} = \left.\frac{\rho_\phi}{\rho_R}\right|_{T_{\rm BBN}} \frac{(a_{\rm BBN}/a_{\rm RH})^{\frac{6k}{k+2}}}{(T_{\rm RH}/T_{\rm BBN})^4}, \tag{3.25}$$

with entropy conservation $g_*(a_{\rm RH})\, T_{\rm RH}^3\, a_{\rm RH}^3 = g_*(a_{\rm BBN})\, T_{\rm BBN}^3\, a_{\rm BBN}^3$ within the SM sector, as well as $\rho_\phi(T_{\rm BBN}) = \frac{7}{8}\left(\frac{4}{11}\right)^{\frac{4}{3}} \Delta N_\nu \frac{\pi^2}{30} T_{\rm BBN}^4$. The resulting bounds for each k are $T_{\rm RH} \lesssim 40\,{\rm MeV}$ ($k=6$), $9\,{\rm MeV}$ ($k=8$), $5\,{\rm MeV}$ ($k=10$), $4\,{\rm MeV}$ ($k=12$) and $3\,{\rm MeV}$ ($14 \le k \le 20$), which we will show as red-shaded regions in the subsequent figures concerning $T_{\rm RH}$. We note that this estimate is in good agreement with a more rigorous treatment performed in ref. [119] using a BBN computing package for the case of kination (large k limit).

The reheating temperature can be determined by solving the Friedmann equation (3.4) for the radiation energy density. This yields [84]

$$\rho_R(a) \simeq \alpha_k \frac{k+2}{8k-14}\sqrt{3} M_P^4 \left(\frac{\rho_{\rm end}}{M_P^4}\right)^{\frac{2k-1}{k}} \left(\frac{a_{\rm end}}{a}\right)^4, \tag{3.26}$$

and evaluating this at $a_{\rm RH}$ we have

$$T_{\rm RH}^4 = \frac{30}{\pi^2\, g_{\rm RH}} M_P^4 \left(\frac{\rho_{\rm end}}{M_P^4}\right)^{\frac{4k-7}{k-4}} \left(\frac{\alpha_k\sqrt{3}\,(k+2)}{8k-14}\right)^{\frac{3k}{k-4}}. \tag{3.27}$$

From eq. (3.27) we find $T_{\rm RH} \simeq 60\,{\rm MeV}$ for $k=10$ and $\rho_{\rm end} \simeq (4.8\times 10^{15}\,{\rm GeV})^4$. Note that, due to the logarithmic dependence of $\phi_{\rm end}$ on k in eq. (2.7), $\rho_{\rm end}$ changes very slowly with k and remains approximately fixed to the above value.

In figure 2, we show in the left panel the reheating temperature for minimal gravitational interactions by the curve labeled $\xi_h = 0$ (other values of ξ_h, non-minimal coupling of the Higgs to the Ricci scalar, are discussed in the next subsection). As one can see, $T_{\rm RH}$ rises to $\simeq 1\,{\rm TeV}$, for $k=20$. This minimal case with $\xi_h = 0$ is excluded by excessive gravitational waves as dark radiation as will be discussed in section 3.5, so a non-minimal coupling is ultimately required.

At the start of the reheating process, the Universe quickly heats to a maximum temperature, $T_{\rm max}$. As discussed in [68], the maximum temperature attained through purely gravitational processes is of order $10^{12}\,{\rm GeV}$, decreasing slightly with k. The maximum radiation density which determines $T_{\rm max}$ was found to be [68]

$$\rho_{\rm max} \simeq \sqrt{3}\,\alpha_k\, M_P^4 \left(\frac{\rho_{\rm end}}{M_P^4}\right)^{\frac{2k-1}{k}} \frac{k+2}{12k-16}\left(\frac{2k+4}{6k-3}\right)^{\frac{2k+4}{4k-7}} \equiv c_*\, T_{\rm max}^4\,. \tag{3.28}$$

Asymptotically at large k, $T_{\rm max} \approx 8\times 10^{11}\,{\rm GeV}$ and $\left(\frac{T_{\rm max}}{T_{\rm RH}}\right)_{k\gg 4} \sim \left(\frac{1}{\alpha_{k\gg 4}}\right)^{1/2}\left(\frac{M_P^4}{\rho_{\rm end}}\right)^{1/2} \gg 1$. This represents a *minimal maximum* temperature, as other process such as decays (not considered here), may lead to a higher maximum temperature. The value of $T_{\rm max}$ is shown in the right panel of figure 2. For minimal gravitational interactions, corresponding to the simple exchange of a graviton, $T_{\rm max} \simeq 10^{12}\,{\rm GeV}$. In fact, as we noted before and

JHEP12(2022)072

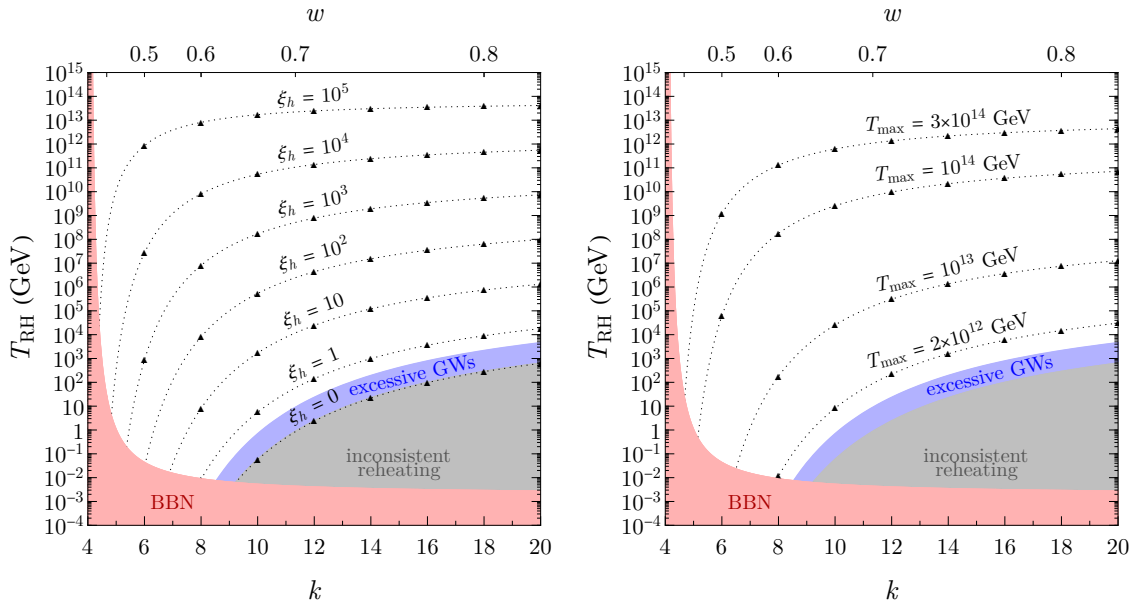

Figure 2. Variation of $T_{\rm RH}$ (left) and $T_{\rm max}$ (right) as a function of k, for different choices of ξ_h. Triangles highlight the physical choices of even k. The red-shaded region is excluded by BBN because low reheating temperatures lead to an excessive inflaton energy density during BBN. The blue-shaded region is similarly excluded by BBN for excessive gravitational waves produced during inflation. The gray-shaded region is excluded as the lowest reheating temperature from gravitational reheating is that from minimal gravity (pure graviton exchange), i.e., $\xi_h = 0$.

will elaborate in section 3.5, gravitational reheating with $\xi_h = 0$ (graviton exchange) is already ruled out by the BBN bound on dark radiation in the form of GWs. Thus, in order to account for the reheating mechanism in a gravitational framework, it is necessary to introduce non-minimal couplings of fields to gravity. We compute the reheating and maximum temperatures for non-minimal gravitational interactions in the next subsection. The value of $T_{\rm max}$ will be relevant when we discuss the DM warmness constraint, because DM is produced relativistically and predominantly at $T_{\rm max}$.

3.4 Non-minimal gravitational production

As pure gravitational particle production can be insufficient, we also consider the possibility that scalar fields have non-minimal couplings to gravity which generate effective couplings between these scalar fields and the RHNs. Thus, we allow both the inflaton ϕ and the Higgs field H to be non-minimally coupled. We denote the complex Higgs doublet as h throughout the following section. One can then write the action as

$$\mathcal{S}_J = \int d^4x\sqrt{-\tilde{g}}\left[-\frac{M_P^2}{2}\,\Omega^2\,\widetilde{\mathcal{R}} + \widetilde{\mathcal{L}}_\phi + \widetilde{\mathcal{L}}_h + \widetilde{\mathcal{L}}_{N_i}\right], \tag{3.29}$$

JHEP12(2022)072

where

$$\widetilde{\mathcal{L}}_\phi = \frac{1}{2}\,\partial_\mu\phi\,\partial^\mu\phi - V(\phi) \tag{3.30}$$

$$\widetilde{\mathcal{L}}_h = \partial_\mu h\,\partial^\mu h^\dagger - V(hh^\dagger) \tag{3.31}$$

$$\widetilde{\mathcal{L}}_{N_i} = \frac{i}{2}\,\overline{\mathcal{N}_i}\overleftrightarrow{\not{\nabla}}\,\mathcal{N}_i - \frac{1}{2}\,M_{N_i}\,\overline{(\mathcal{N})^c}_i\,\mathcal{N}_i + \widetilde{\mathcal{L}}_{\rm yuk} \tag{3.32}$$

$$\widetilde{\mathcal{L}}_{\rm yuk} = -y_{N_i}\,\overline{\mathcal{N}_i}\,\widetilde{h^\dagger}\,\mathbb{L} + \text{h.c.}\,, \tag{3.33}$$

where $\mathcal{N}\,,\mathbb{L}$ are the RHN and SM lepton doublet fields in Jordan frame. The conformal factor Ω^2 is given by

$$\Omega^2 \equiv 1 + \frac{\xi_\phi\,\phi^2}{M_P^2} + \frac{\xi_h\,|h|^2}{M_P^2}\,. \tag{3.34}$$

It is convenient to remove the non-minimal couplings by performing the redefinition of the metric field via the usual conformal transformation from the Jordan frame to the Einstein frame,

$$g_{\mu\nu} = \Omega^2\,\tilde{g}_{\mu\nu}\,, \tag{3.35}$$

$$\begin{aligned}\mathcal{S}_E = \int d^4x\sqrt{-g}\Bigg[&-\frac{M_P^2\,\mathcal{R}}{2} + \frac{K^{ab}}{2}\,g^{\mu\nu}\partial_\mu S_a\,\partial_\nu S_b + \frac{i}{2\,\Omega^3}\,\overline{N_i}\overleftrightarrow{\not{\nabla}}\,N_i - \frac{1}{\Omega^4}\left(\frac{M_{N_i}}{2}\,\overline{N_i^c}\,N_i + \mathcal{L}_{\rm yuk}\right)\\ &- \frac{3i}{4\Omega^4}\,\overline{N_i}\left(\overleftrightarrow{\not{\partial}}\,\Omega\right)N_i - \frac{1}{\Omega^4}\,(V_\phi + V_h)\Bigg]\,,\end{aligned} \tag{3.36}$$

where we have used

$$\sqrt{-\tilde{g}} \to \frac{\sqrt{-g}}{\Omega^4} \tag{3.37}$$

$$\tilde{\not{\nabla}} \to \Omega\not{\nabla} - \frac{3}{2}\Omega^2(\not{\partial}\Omega)\,, \tag{3.38}$$

and the indices a, b enumerate the fields ϕ, and the real components of h. Then making spinor field redefinition $L \to \Omega^{3/2}L$, $N_i \to \Omega^{3/2}N_i$ and $\overline{N_i} \to \Omega^{3/2}\overline{N_i}$ we recover the following action with canonical kinetic term for the RHN

$$\begin{aligned}\mathcal{S}_E = \int d^4x\sqrt{-g}\Bigg[&-\frac{M_P^2\,\mathcal{R}}{2} + \frac{K^{ab}}{2}\,g^{\mu\nu}\partial_\mu S_a\,\partial_\nu S_b - \frac{1}{\Omega^4}\,(V_\phi + V_h) + \frac{i}{2}\,\overline{N_i}\overleftrightarrow{\not{\nabla}}\,N_i\\ &- \frac{1}{2\,\Omega}\,M_{N_i}\,\overline{N_i^c}\,N_i + \frac{1}{\Omega}\,\mathcal{L}_{\rm yuk}\Bigg]\,.\end{aligned} \tag{3.39}$$

The kinetic function is given by

$$K^{ab} = 6\,\frac{\partial\log\Omega}{\partial S_a}\frac{\partial\log\Omega}{\partial S_b} + \frac{\delta^{ab}}{\Omega^2}\,. \tag{3.40}$$

In what follows, we will be interested in the small-field limit

$$\frac{|\xi_\phi|\phi^2}{M_P^2},\ \frac{|\xi_h||h|^2}{M_P^2} \ll 1\,. \tag{3.41}$$

JHEP12(2022)072

Since we necessarily consider large field values for the inflaton coming out of inflation, this constrains $\xi_\phi \ll 1$. However, there is no such constraint on ξ_h which can take relatively large values.

Expanding the kinetic and potential terms in the action in eq. (3.39) in powers of $1/M_P^2$, we obtain a canonical kinetic term for the scalar fields, and deduce the leading-order interactions between scalars and the RHNs induced by the non-minimal couplings. Note that, the non-minimally coupled Yukawa interaction in eq. (3.39) gives rise to a 3-to-2 (or 2-to-3) process with RHN in the final state above electroweak symmetry breaking temperature. These processes thus will be kinematically suppressed and have a subdominant contribution to the RHN yield. The kinetic terms for the RHNs can be expressed in the form

$$\mathcal{L}_{\rm non-min.} = -\sigma^{\xi}_{hN_i} |h|^2 \overline{N_i^c} N_i - \sigma^{\xi}_{\phi N_i} \phi^2 \overline{N_i^c} N_i \,, \tag{3.42}$$

with

$$\sigma^{\xi}_{\phi N_i} = \frac{M_{N_i}}{2M_P^2} \xi_\phi \tag{3.43}$$

$$\sigma^{\xi}_{hN_i} = \frac{M_{N_i}}{2M_P^2} \xi_h \,. \tag{3.44}$$

These non-minimal interactions open up additional channels [68]

- RHN production from inflaton scattering: $\phi\phi \to N_i\, N_i$
- RHN production from Higgs scattering: $hh^\dagger \to N_i\, N_i$
- Higgs production from inflaton scattering: $\phi\phi \to hh^\dagger$.

Interestingly, as can be seen from the interaction terms, the production of RHNs is systematically proportional to the mass of the fermion. Then, for the thermal production of RHNs, the production rate is

$$R^{T,\xi}_{N_i} \simeq N_h \, \frac{\zeta(3)^2 \, \xi_h^2}{32\,\pi^5} \, \frac{M_{N_i}^2 \, T^6}{M_P^4} \,, \tag{3.45}$$

where $\zeta(x)$ is the Riemann-zeta function. For both minimal and non-minimal gravitational couplings, the leading term in the production rate for scalar dark matter scales as T^8 [69]. Similarly, the production rate for fermions in minimal gravity also scales as T^8 as seen in eq. (3.1). However, for non-minimal gravitational interactions, after the conformal rescaling to obtain canonical kinetic terms, there is no non-minimal coupling to the kinetic terms (in contrast to the scalars where this coupling is found in eq. (3.39)). Instead, we are left with only the mass term coupled to $|h|^2$ and the thermal production rate is proportional only to $\propto M_{N_i}^2 T^6$.

JHEP12(2022)072

Using the rate in eq. (3.45) we obtain the number density at the end of reheating due to the non-minimal interaction as

$$n_{N_i}^{T(\xi_h\neq 0)} = \left(\frac{\sqrt{3}\,N_h\,\zeta(3)^2\,\xi_h^2}{32\,\pi^5\,c_*^{3/2}}\,\frac{M_{N_i}^2\,\rho_{\rm RH}}{M_P^3}\right)\frac{(k+2)\left(1-\left(\frac{\rho_{\rm end}}{\rho_{\rm RH}}\right)^{\frac{7}{3k}-\frac{4}{3}}\right)^{-3/2}}{72\,(5-4k)\,\Gamma\left(\frac{29-20k}{14-8k}\right)}$$
$$\times\left[9\sqrt{\pi}(5-4k)\left(\frac{\rho_{\rm end}}{\rho_{\rm RH}}\right)^{1/k}\Gamma\left(\frac{4k-4}{4k-7}\right)+4\left(\frac{\rho_{\rm end}}{\rho_{\rm RH}}\right)^{\frac{16k^2+4k+169}{21k-12k^2}}\Gamma\left(\frac{29-20k}{14-8k}\right)\mathcal{G}\right], \tag{3.46}$$

with

$$\mathcal{G}=\left(\frac{\rho_{\rm end}}{\rho_{\rm RH}}\right)^{\frac{4(k+30)}{3k(4k-7)}}\left[3(4k-5)\left(\frac{\rho_{\rm end}}{\rho_{\rm RH}}\right)^{\frac{16k^2+49}{3k(4k-7)}}-6\left(\frac{\rho_{\rm end}}{\rho_{\rm RH}}\right)^{\frac{56}{3(4k-7)}}\right]{}_2F_1(\ldots)\,,$$

where ${}_2F_1\left(-\frac{1}{2},\frac{3}{4k-7},\frac{4k-4}{4k-7},\left(\frac{\rho_{\rm end}}{\rho_{\rm RH}}\right)^{\frac{7}{3k}-\frac{4}{3}}\right)$ is the hypergeometric function.

For the inflaton scattering process $\phi\phi\to N_i\,N_i$, on the other hand, we find

$$R_{N_i}^{\phi,\xi}=\frac{M_{N_i}^2\,\xi_\phi^2\,\phi_0^4\,\omega^2}{32\pi M_P^4}\sum_{n=1}^{\infty}(2n)^2|\mathcal{Q}_{2n}^{(2)}|^2\times\sqrt{1-\frac{4M_{N_i}^2}{E_{2n}^2}}\,, \tag{3.47}$$

where we define $\phi_0=\left(\frac{\rho_\phi}{\lambda\,M_P^{4-k}}\right)^{\frac{1}{k}}$ and $\mathcal{Q}_n^{(2)}$ by

$$\phi^2(t)=\phi_0^2(t)\cdot\mathcal{Q}^2(t)=\phi_0^2(t)\sum_{n=-\infty}^{\infty}\mathcal{Q}_n^{(2)}e^{-in\omega t}\,. \tag{3.48}$$

This rate is restricted by the small field limit that imposes a stringent bound on ξ_ϕ from $\sqrt{|\xi_\phi|}\lesssim M_P/\langle\phi\rangle$. In particular, at the beginning of inflaton oscillations $\langle\phi\rangle\sim M_P$ and $|\xi_\phi|\lesssim 1$. When we compare this rate with the one due to inflaton scattering mediated by minimal gravitational interactions (eq. (3.16)), we obtain

$$\frac{R_{\phi N_i}^{\phi,\xi}}{R_{N_i}^{\phi^k}}\approx\left[\frac{k\,(k-1)\,\xi_\phi\,(\omega/m_\phi)^2}{\sqrt{8}}\right]^2\frac{\sum_{n=1}^{\infty}(2n)^2|\mathcal{Q}_{2n}^{(2)}|^2}{\sum_{n=1}^{\infty}\frac{1}{(2n)^2}\,|\mathcal{P}_{2n}^k|^2}\,. \tag{3.49}$$

This ratio takes values between $\{32\,\xi_\phi^2,\,242\,\xi_\phi^2\}$ for $k\in[6,20]$. Hence, the non-minimal contribution from inflaton scattering dominates over the graviton exchange for $\xi_\phi>\frac{1}{2\sqrt{8}}$ when $k=6$ and for $\xi_\phi>0.06$ when $k=20$. In what follows, we will neglect this contribution as it dominates for values of ξ_ϕ close to the small field limit, making the assumption of canonical kinetic terms of the fields invalid.

The non-minimal coupling of Higgs bosons to gravity provides an additional channel to reheat the Universe through gravitational processes, with the following rate [84]

$$(1+\omega_\phi)\Gamma_\phi=R_H^{\phi,\xi}\simeq\frac{\xi_h^2N_h}{4\pi M_P^4}\sum_{n=1}^{\infty}2n\omega\left|2\times\mathcal{P}_{2n}^k\rho_\phi+\frac{(n\omega)^2}{2}\phi_0^2|\mathcal{Q}_n|^2\right|^2=\alpha_k^\xi M_P^5\left(\frac{\rho_\phi}{M_P^4}\right)^{\frac{5k-2}{2k}}\,, \tag{3.50}$$

JHEP12(2022)072

where $\mathcal{Q}_n$ has been defined in eq. (3.15) and α_k^ξ is given in table 1. If we solve eq. (3.4) for ρ_R, the reheating temperature in the presence of the non-minimal coupling is then given by

$$\left(T_{\rm RH}^\xi\right)^4 = \frac{30}{\pi^2\, g_{\rm RH}}\, M_P^4 \left(\frac{\rho_{\rm end}}{M_P^4}\right)^{\frac{4k-7}{k-4}} \left(\frac{\alpha_k^\xi\,\sqrt{3}\,(k+2)}{8k-14}\right)^{\frac{3k}{k-4}} . \tag{3.51}$$

The reheating temperature as a function of k is shown in the left panel of figure 2 for several values of ξ_h. The maximum temperature in this case is determined from

$$\rho_{\rm max}^\xi \simeq \sqrt{3}\,\alpha_k^\xi\, M_P^4 \left(\frac{\rho_{\rm end}}{M_P^4}\right)^{\frac{2k-1}{k}} \frac{k+2}{12k-16} \left(\frac{2k+4}{6k-3}\right)^{\frac{2k+4}{4k-7}} \equiv c_*\,(T_{\rm max}^\xi)^4 . \tag{3.52}$$

Contours of $T_{\rm max}^\xi$ in the $(k, T_{\rm RH})$ plane are shown in the right panel of figure 2, where the appropriate values of ξ_h taken from the left panel are used to calculate $T_{\rm max}^\xi$.

3.5 Gravitational waves generated during inflation

In this section, we review the calculation of gravitational waves generated by quantum fluctuations during inflation, followed by a cosmological era where the inflaton energy dominates and redshifts faster than radiation. This results in an enhancement of gravitational waves, which places a constraint from excessive gravitational waves as dark radiation and offers a gravitational wave signal with a distinctive spectrum.

The ratio of the gravitational wave (GW) energy density to that of the radiation bath is given by [120]

$$\frac{\rho_{\rm GW}}{\rho_R} = \frac{1}{32\pi G\rho_R}\frac{k_{\rm GW}^2}{2}\mathcal{P}_T(k_{\rm GW}) \quad \text{with} \quad \mathcal{P}_T(k_{\rm GW}) \equiv \frac{2H_I^2(k_{\rm GW})}{\pi^2 M_P^2} , \tag{3.53}$$

where $k_{\rm GW}$ is the momentum mode of the GW, $\mathcal{P}_T$ is the primordial tensor power spectrum, $H_I(k_{\rm GW})$ is the Hubble scale during inflation when the mode $k_{\rm GW}$ exits the horizon, $T_{\rm hc}$ is the horizon-crossing temperature when the mode re-enters the horizon at $k_{\rm GW} = H(T_{\rm hc})$, and the factor of $1/2$ accounts for the time average of the rapidly oscillating metric perturbations. In our case, $\rho_{\rm GW}/\rho_R$ is redshift invariant up to the change of g_* after $T = T_{\rm max}$ because entropy is only efficiently produced at $T = T_{\rm max}$ as discussed in section 3.3. Therefore, the final gravitational wave strength is given by $\Omega_{\rm GW}h^2 = \Omega_\gamma\, h^2\,(\rho_{\rm GW}/\rho_R) \times \left[g_{*s}^4({\rm eV})/g_*(T_{\rm hc})g_*^3({\rm eV})\right]^{\frac{1}{3}}$ where $\Omega_\gamma = \rho_{\gamma,0}/\rho_{{\rm crit},0}$ is the fraction of the photon energy density today. Here $g_{*s}({\rm eV}) = \left[2 + \frac{7}{8}\times 2\times 3\times\left(\frac{4}{11}\right)\right] \simeq 3.91$ and $g_*({\rm eV}) = \left[2 + \frac{7}{8}\times 2\times 3\times\left(\frac{4}{11}\right)^{4/3}\right] \simeq 3.36$ denote the effective number of relativistic degrees of freedom relevant for the entropy density and the energy density, respectively.

As one can see, if horizon crossing occurs during radiation domination $k_{\rm GW}^2 = H^2(T_{\rm hc}) = \rho_R/(3M_P^2)$, then the GW spectrum becomes scale invariant. On the other hand, if horizon crossing occurs during the inflaton-dominated era, the GW strength is enhanced by a factor of ρ_ϕ/ρ_R evaluated at $T_{\rm hc}$. As a result, the largest enhancement is for the mode that re-enters the horizon right after inflation at $T_{\rm max}$. For minimal gravitational reheating ($\xi_h = 0$), the enhancement in this mode is $\rho_{\rm end}/\rho_R(T_{\rm max}) \simeq (4\text{–}6)\times 10^{13}$ for $k \in [6, 20]$,

JHEP12(2022)072

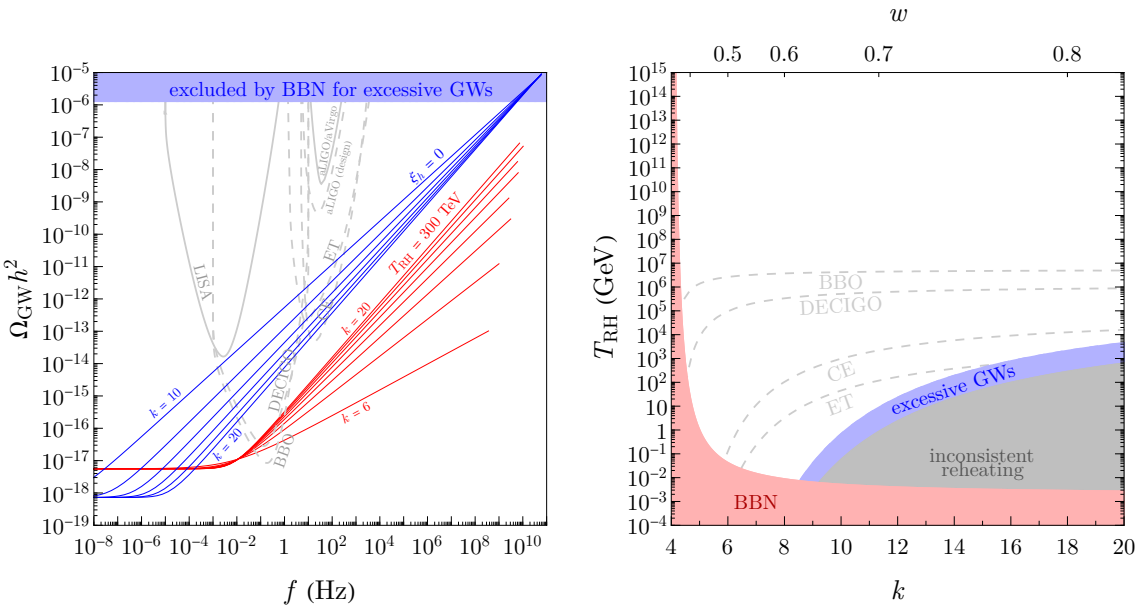

Figure 3. Gravitational wave constraints and future prospects. Left: the blue-shaded region is excluded by BBN for excessive dark radiation. The blue and red curves fix $\xi_h = 0$ and $T_{\rm RH} = 300\,\text{TeV}$, respectively. Various curves of the same color use different values of k as labeled and in increments of 2. The sensitivity of several future experiments as a function of frequency is also shown. Right: the blue region is excluded by BBN for the excessive GW energy as dark radiation. The regions below the gray dashed curves can be probed by the GW experiments as specified.

based on eqs. (2.5) and (2.7). This gives $\Omega_{\rm GW}h^2 \simeq (8\text{–}10) \times 10^{-6}$, which corresponds to the high frequency points of the blue curves, which fix $\xi_h = 0$, in the left panel of figure 3. These values are excluded by the BBN bound of $\Omega_{\rm GW}h^2 \simeq 1.3 \times 10^{-6}$ [118], shown by the blue-shaded region at the top. Therefore, the case with minimal gravitational interactions is excluded, which was previously pointed out by ref. [87]. The constraint is relaxed when $T_{\rm max}$ is increased, e.g., by non-minimal gravitational interactions via ξ_h [cf. eq. (3.52)], because the GW energy density relative to that of radiation is smaller in this case. The blue region in the right panel of figure 3 (and subsequent figures) shows the constraint in this non-minimal scenario, which excludes $\xi_h \lesssim 0.5$, as can be seen from the left panel of figure 2. Alternatively, ref. [121] offers the solution where the inflaton energy is more efficiently transferred to radiation via a tachyonic growth of a new field.

In addition to setting a constraint, such enhanced gravitational waves offer an exciting signature to search for [122]. The amount of enhancement depends on ρ_ϕ/ρ_R at the time of horizon crossing, implying that the GW spectrum depends on k via ρ_ϕ. By analyzing modes that re-enter the horizon after $T_{\rm max}$ and using $\rho_\phi \propto a^{-6k/(k+2)}$ from eq. (3.5), we find the GW spectrum scales with the frequency as $\Omega_{\rm GW}h^2 \propto f^{\frac{k-4}{k-1}}$, which is consistent with ref. [87]. The enhanced GW spectra are demonstrated in the left panel of figure 3 for the different values of k in the blue and red curves. The blue (red) curves correspond to the minimal scenario ($T_{\rm RH} = 300\,\text{TeV}$), and allow for k to vary from 10 (6) to 20 in increments of 2 (for $\xi_h = 0$, $k < 10$ is excluded by BBN for low $T_{\rm RH}$ according to figure 2). Here, the

JHEP12(2022)072

frequency is obtained by redshifting the initial momentum mode at $T_{\rm hc}$ to today's photon temperature $T_{\gamma,0}$ as

$$f = \frac{k_{\rm GW}}{2\pi} \frac{T_{\gamma,0}}{T_{\rm hc}} \left(\frac{g_*(\text{eV})}{g_*(T_{\rm hc})} \right)^{\frac{1}{3}} . \tag{3.54}$$

Therefore, by measuring the slope of $\Omega_{\rm GW}h^2$ as a function f, one can determine k and thus reveal the shape of the inflaton potential energy near the minimum. Note that, the end-point frequencies for the red curves are different for different choices of k (and different ξ_h), as for a given k and $T_{\rm RH}$, the maximum possible frequency is dictated by

$$f_{\rm max} = \frac{H(T_{\rm max})}{2\pi} \frac{a_{\rm end}}{a_0} , \tag{3.55}$$

which for $\xi_h = 0$ turns out to be $\simeq 7 \times 10^{10}$ Hz for all k, while modes with frequencies $f > f_{\rm max}$ are never produced. In the right panel of figure 3, the regions below the gray dashed curves can be probed by the future gravitational wave observatories — BBO [123–125], DECIGO [126–128], CE [129, 130] and ET [131–134]. Here we use the sensitivity curves derived in ref. [135]. Since these GW observatories probe frequencies that correspond to modes that exit the horizon early in the inflation period, we use the large-field asymptotic value of $V(\phi)$ in eq. (2.5) to obtain H_I. In the left panel of figure 3, we illustrate the GW spectra in the red curves for a fixed $T_{\rm RH} = 300\,\text{TeV}$, which can be detected by DECIGO for $k \geq 8$ and by BBO for all $k \geq 6$. Remarkably, in the right panel, a large region in the parameter space with $T_{\rm RH} < 5 \times 10^6\,\text{GeV}$ can be probed by future GW detectors. We emphasize that this potential GW signal is generic for our model and applicable throughout this work, although we do not show these sensitivity curves in subsequent figures for clarity of presentation.

4 Results and discussion

4.1 A stable DM candidate

As we have seen from the previous two subsections, for each value of k and ξ_h (in the non-minimal case), there is a unique value for $T_{\rm RH}$. These are shown in the left panel of figure 2. The gravitational thermal production of DM generally requires reheating temperatures much larger than can be obtained with $\xi_h = 0$. In this section, we will consider $T_{\rm RH}$ and k as free parameters and it should be understood that we are implicitly assuming that $\xi_h \neq 0$ and takes the necessary value to achieve a particular reheating temperature for a given value of k. For the production of DM, both minimal and non-minimal thermal contributions are included, whereas for the generation of a lepton asymmetry only minimal contributions from inflaton scattering are considered.

The results presented in this section depend on the underlying class of inflationary models. As noted earlier, we consider T-models of inflation [88] for which we have determined λ and $\rho_{\rm end}$. As discussed above, there are two contributions to the DM relic density: from gravitational scattering within the newly formed primordial plasma and directly from inflaton

JHEP12(2022)072

scattering. These two contributions are presented separately in the upper two panels of figure 4. In the upper left panel, we show two contours of the yield, $n_{N_1}/s = 10^{-22}$ and 10^{-24}, for both minimal gravitational interactions (dotted curves) using eq. (3.11) and non-minimal interactions (dot-dashed curves) using eq. (3.46).[9] Note the latter yield is proportional to $M_{N_1}^2$ as shown by the contour labels, and we have normalized these contours by choosing $M_{N_1} = 10^8\,\text{GeV}$. Also note, $M_{N_1} n_{N_1}/s \simeq 0.44\,\text{eV}$ is needed to explain the observed dark matter density, $\Omega_{N_1} h^2 = 0.12$. For $k > 4$ and minimal gravitational interactions, the relic density increases with reheating temperature, $n_{N_1}/s \sim T_{\rm RH}^{\frac{5k-20}{3k}}$. The scaling of n_{N_1}/s for non-minimal interactions is more complicated but also increases with $T_{\rm RH}$.

In the upper right panel of figure 4, we provide four contours of the yield, n_{N_1}/s, produced from inflaton scattering, which also scales as $M_{N_1}^2$. The gravitational production process from inflaton scattering is complementary to the thermal production process just discussed. Recall that we are assuming ξ_ϕ is small enough that non-minimal scattering processes can be ignored. In this case, from eq. (3.19), we see that $n_{N_1}/s \sim T_{\rm RH}^{-1+\frac{4}{k}}$ and for $k > 4$, the relic density decreases with increasing $T_{\rm RH}$. Recalling that $M_{N_1} n_{N_1}/s \simeq 0.44\,\text{eV}$ is needed to explain the observed DM density, $\Omega_{N_1} h^2 = 0.12$, we find indeed that higher reheating temperatures require *lighter* DM candidates to fit with the relic abundance constraint.

Combining the two constraints shown in the top panels of figure 4 we see that for a given k and M_{N_1}, there are both upper (from thermal scattering) and lower (from inflaton scattering) limits to $T_{\rm RH}$ so as to avoid exceeding the observed cold DM abundance. The resulting relic density as a function of $T_{\rm RH}$ is shown in the bottom left panel of figure 4, where we show the total relic abundance $(\Omega_{N_1}^T + \Omega_{N_1}^{\phi^k})\,h^2$ relative to the observed abundance for a fixed $k = 14$ and three choices of the DM mass $M_{N_1} = \{10^6, 10^7, 10^8\}\,\text{GeV}$. We clearly see that the desired relic density ($\Omega_{N_1} = 0.12$) is obtained *twice*: (i) at a lower reheating temperature, where inflaton scattering dominates, and (ii) for a higher reheating temperature, when we are in the thermal production regime. The allowed region corresponds to the parameter space at or *below* the line $\Omega h^2/0.12 = 1$ in the bottom left panel of figure 4. For $M_{N_1} > 3 \times 10^8\,\text{GeV}$, there are no values of ($T_{\rm RH}$, k) that result in an acceptable density of DM, and the allowed range in $T_{\rm RH}$ is larger with lighter DM. This is understandable as, the thermal relic requiring a *larger upper bound* on $T_{\rm RH}$ for lighter DM, while the inflaton scattering requires a *smaller lower bound* on $T_{\rm RH}$ for lighter DM.

A two-dimensional version of the lower left panel of figure 4, over a range in k, is shown in the lower right panel. Low values of $T_{\rm RH}$ are excluded by BBN. Once again, the gray-shaded region in the lower right corner of this panel is also excluded since minimal gravitational interactions would produce a reheating temperature larger than the values in that region. Within each shaded band (the color corresponds to a specific choice of M_{N_1}), the total relic density is below the observed DM density. The observed value is reached on the border of the colored bands. For DM of masses very close to 1 PeV, there exists a viable parameter space for $k \geq 9$ (along the boundary of the excessive GWs region), requiring

[9] Note that minimal gravitational interactions ($\xi_h = 0$) are not actually possible at these reheating temperatures which require $\xi_h \neq 0$.

JHEP12(2022)072

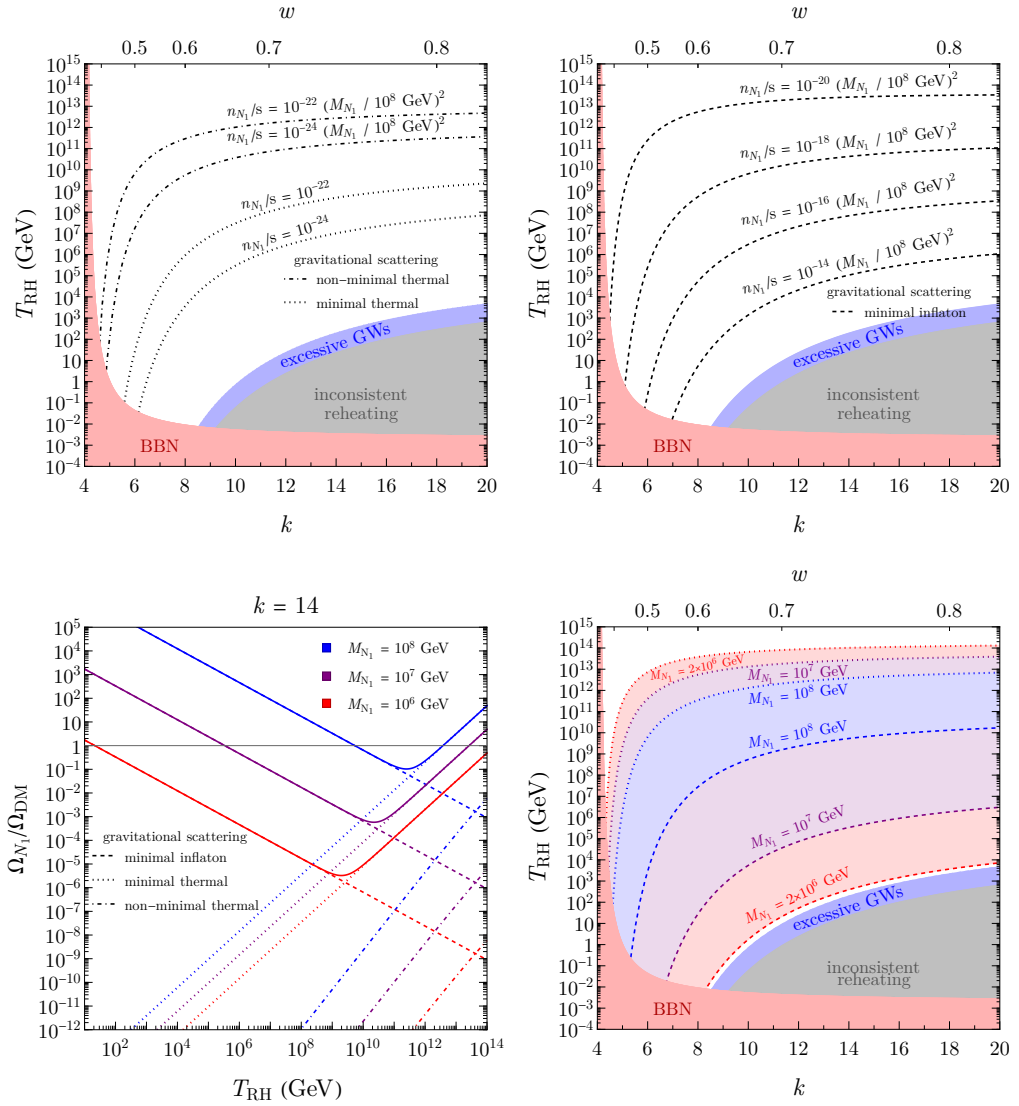

Figure 4. Top left: contours of fixed comoving number density, $n_{N_1}/s = 10^{-22}$ and 10^{-24} in the $(k, T_{\rm RH})$ plane. $M_{N_1} n_{N_1}/s \simeq 0.44\,{\rm eV}$ is needed to explain the observed dark matter density, $\Omega_{N_1} h^2 = 0.12$. Dotted curves assume DM production solely from minimal gravitational scattering in the thermal bath. Dot-dashed curves correspond to non-minimal gravitational scatterings. The latter are scaled with $M_{N_1}^2$. Top right: contours of $n_{N_1}/s = 10^{-20}, 10^{-18}, 10^{-16}$ and 10^{-14} each scaled with $M_{N_1}^2$ assuming DM production only from inflaton scattering. In both upper panels, the gray-shaded region is excluded as minimal gravitational interactions necessarily produce larger reheating temperatures. Low reheating temperatures shaded in red (blue) are excluded by BBN for an excessive inflaton (GW) energy. Bottom left: the total relic abundance $(\Omega_{N_1}^T + \Omega_{N_1}^{\phi^k})h^2/0.12$ as a function of reheating temperature for three choices of DM masses $\{10^6, 10^7, 10^8\}$ GeV for fixed $k = 14$. Individual contributions to the dark matter density are distinguished by line types as indicated. Bottom right: coloured regions correspond to values of $(k, T_{\rm RH})$ with $(\Omega_{N_1}^T + \Omega_{N_1}^{\phi^k})h^2 \leq 0.12$ for the three choices of M_{N_1} used in the bottom left panel, and the lines styles indicate the dominant contribution.

JHEP12(2022)072

$\xi_h \simeq 0.5$. For larger masses, the range in k extends to lower values, and higher reheating temperatures are possible and require larger non-minimal coupling to gravity.

Having identified the regions of the $(k, T_{\rm RH})$ parameter space with a suitable DM density, we turn to the production of the baryon asymmetry through gravitationally induced leptogenesis. This analysis was performed in [84] and therefore we only briefly summarize the results found there. We note, however, ref. [84] neglected the kinematic suppression in eq. (3.17) to maintain the model independence of the analysis, though this effect is included in the present work. In figure 5, we show contours of some benchmark values of the mass of N_2 that reproduce the observed baryon asymmetry $Y_B^{\rm obs}$. We find that the gravitational contribution to the baryon asymmetry is essentially entirely due to inflaton scattering rather than the thermal particles in the SM bath. Since minimal gravitational interactions are excluded by excessive GWs, non-minimal interactions are required to produce a sufficiently large thermal bath so that GW fractional energy is consistent with BBN. Leptogenesis via N_2 is therefore possible above the border of the blue-shaded region in figure 5, indicating a mass $M_{N_2} \gtrsim 3 \times 10^{11}\,\text{GeV}$ is required. Larger values of M_{N_2} can produce the correct asymmetry so long as $\xi_h > 0$. Nonetheless, when $M_{N_2} \gtrsim 3 \times 10^{12}\,\text{GeV}$, the baryon asymmetry starts to become suppressed for the following reason. The inflaton mass obtained from eqs. (2.5) and (2.7), $m_\phi \simeq 1.2 \times 10^{13}\,\text{GeV}$ across all k values, is no longer much larger than M_{N_2} and the kinematic suppression in eq. (3.17) becomes important. This explains the existence of the green region as well as why the curve for $M_{N_2} = 10^{13}\,\text{GeV}$ is at a lower $T_{\rm RH}$ than that for $M_{N_2} = 3 \times 10^{12}\,\text{GeV}$. Once again, the bottom red region is forbidden by BBN because of an excessive inflaton energy density during BBN. In summary, we observe that, saturating the bound on GWs from BBN, together with the right DM abundance and successful leptogenesis requires $\xi_h \simeq 0.5$, $M_{N_2} \simeq 3 \times 10^{11}\,\text{GeV}$ and $M_{N_1} \simeq 10^6\,\text{GeV}$. As discussed above, this parameter space can be extended, allowing larger values $\{M_{N_1}, M_{N_2}\}$ if one considers stronger non-minimal gravitational couplings by $\xi_h \gtrsim 0.5$, thus allowing a larger reheating temperature [cf. eq. (3.51)].

Combining our preceding analyses, it is possible, for a given $V(\phi)$, to constrain the $(M_{N_1}, M_{N_2}, \xi_h)$ parameter space by requiring leptogenesis, DM production and reheating to have a common gravitational origin. Indeed, for a given k and DM mass M_{N_1}, the temperature $T_{\rm RH}$ can be determined by the relic abundance constraint. In turn, $T_{\rm RH}$ determines the value of ξ_h needed to reheat the Universe, as well as the value of M_{N_2} which gives the desired baryon asymmetry through leptogenesis. To illustrate our result, we project the viable parameter space in the (M_{N_1}, M_{N_2}) plane in figure 6 for different values of ξ_h, allowing k to vary within $k \in [6, 20]$. In each coloured line segment, gravitational interactions are responsible for the observed DM relic abundance, the baryon asymmetry and reheating. Different coloured slanted line segments in this figure correspond to different choices of the non-minimal coupling ξ_h, with $\xi_h = 0$ being ruled out from overproduction of GWs. The maximum possible value for ξ_h is around 13.5, above which the mass M_{N_2} necessary to reproduce the observed baryon asymmetry gets too close to m_ϕ and kinematic suppression becomes significant, as can be seen from figure 5. Note that for each ξ_h, the allowed parameter space satisfying all the constraints, is rather restricted. This is better seen from the right panel figure, where we have zoomed in to the $\xi_h = 1$ case. Interestingly,

JHEP12(2022)072

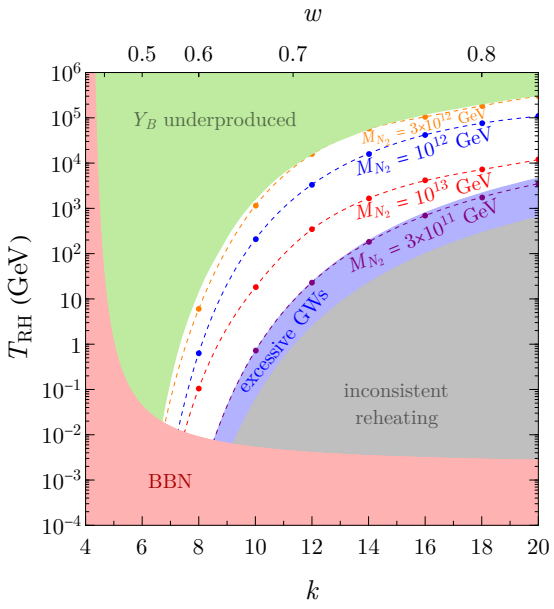

Figure 5. Contours of M_{N_2} corresponding to the observed baryon asymmetry [cf. eq. (3.24)] in the $(k, T_{\rm RH})$ plane. The red-shaded region correspond to the lower bound on $T_{\rm RH}$ from BBN, and the green region leads to underproduction of Y_B due to the kinematic suppression in inflaton scattering when M_{N_2} approaches m_ϕ.

this shows that the viable parameter space is approximately independent of k, while $k = 6$ and 8 are excluded by BBN as can be seen from the left panel of figure 2.

4.2 The case for a decaying gravitational DM & IceCube events

Until now, we have assumed that the DM candidate, N_1, is absolutely stable. If it is not, and N_1 has non-zero Yukawa components, y_{1i}, N_1 can decay to SM final states. In this case, one necessary (but not sufficient) constraint on the DM mass and Yukawa coupling arises from the requirement of having a lifetime larger than the age of the Universe $\tau_{N_1} \gtrsim \tau_{\rm univ} \simeq 4.35 \times 10^{17}$ s. On the other hand, the IceCube detector has reported the detection of three PeV neutrinos, a roughly 3σ excess above expected background rates [136–138]. The three highest energy events correspond to deposited energies of 1.04 PeV, 1.14 PeV and 2.0 PeV. Although the origin of these very high energy events is still unclear, it has been shown in refs. [42, 139–152] that such events could be sourced from the decays of superheavy DM particles. The neutrino energy spectrum presents a high-energy cutoff at $m_{\rm DM}/2$ [140, 141] if two body decays including one neutrino are present. The total excess can be interpreted as high energy neutrinos resulting from the decay of N_1 with $\tau_{N_1} \approx 10^{28}$ s for both normal and inverted hierarchies [140, 153]. Given that the maximum energy of the IceCube events has been measured to be about 2 PeV, the mass of the DM particle is constrained to be $\simeq 4$ PeV. Moreover, the IceCube spectrum sets a lower bound on the DM lifetime of the order of 10^{28} s [141, 153], which is approximately model-independent and orders of magnitude larger than the lifetime of the Universe. Thus, satisfying this bound automatically makes N_1 a nearly stable relic, and hence a good DM candidate. For

JHEP12(2022)072

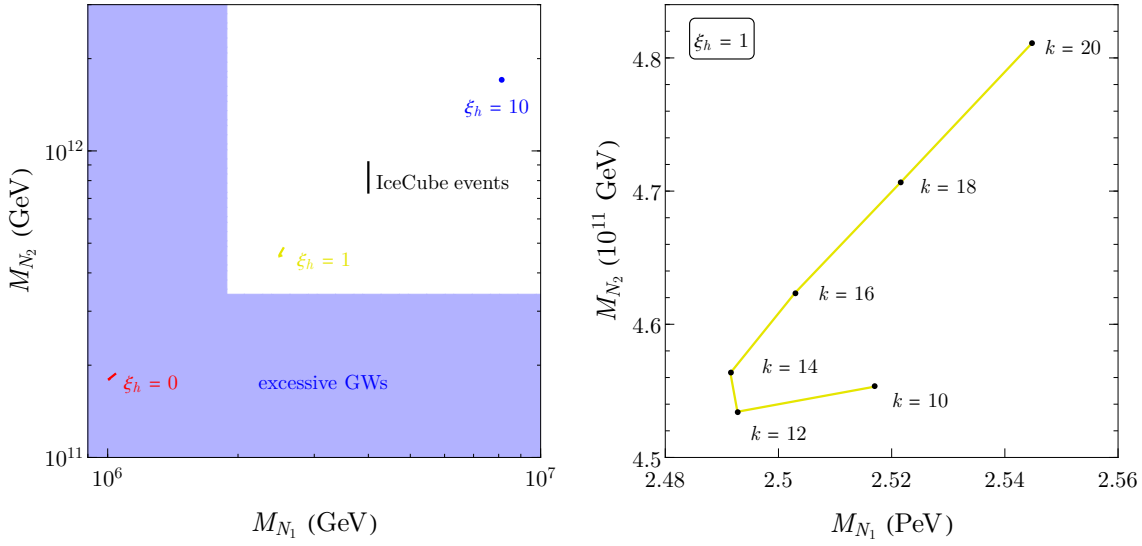

Figure 6. Viable parameter space in the (M_{N_1}, M_{N_2}) plane for which gravitational interactions are responsible for the observed DM relic abundance (in N_1), the baryon asymmetry (produced from N_2 decays), and reheating for $k \in [6, 20]$. In the left panel, different colours correspond to $\xi_h = \{0, 1, 10\}$ diagonally from bottom left (red) to top right (blue). The vertical black segment indicates the range in M_{N_2} for $M_{N_1} = 4\,\text{PeV}$ for the range in k considered, where the connection to the IceCube high-energy neutrino excess will be discussed in the next subsection. In the right panel, we magnify the parameter space for a fixed non-minimal coupling $\xi_h = 1$. The dots correspond to even values of k as indicated.

$N_1 \to \ell\, H$ decay, we find

$$\tau \equiv \Gamma^{-1}_{N_1 \to \ell\, H} \simeq \left(\frac{y^2_{N_1} M_{N_1}}{8\,\pi}\right)^{-1} \simeq 10^{28}\ \text{s} \left(\frac{4\times 10^{-29}}{y_{N_1}}\right)^2 \left(\frac{1\,\text{PeV}}{M_{N_1}}\right)\,; \tag{4.1}$$

that is, the Yukawa coupling y_{N_1} must be highly suppressed.

On the other hand, in order to satisfy the observed DM abundance via the freeze-in mechanism in the early Universe through inverse decay: $\nu\,, H \to N_1$ involving the same Yukawa, one needs [32, 150]

$$\Omega_{N_1}\, h^2 \simeq 0.12 \left(\frac{y_{N_1}}{1.2\times 10^{-12}}\right)^2 \left(\frac{M_{N_1}}{1\,\text{PeV}}\right)\,. \tag{4.2}$$

This means that the Yukawa required to interpret the PeV IceCube event from the decay of N_1, $y_{N_1} \sim 10^{-29}$, is far too small for the thermal bath to populate the Universe from the freeze in mechanism. Thus, if we are restricted to dimension-four interactions involving RHN and the SM, it is not possible to simultaneously explain the DM relic density and the IceCube events. Alternatively, we may consider higher dimensional operators [150], modified gravity/cosmology [154] or some different production mechanism for DM [155].

Our minimalistic framework contains a natural avenue to reconcile both the DM abundance and IceCube events, through the gravitational production of decaying PeV neutrinos in the early Universe. However, as discussed in section 3.5, the case with minimal

JHEP12(2022)072

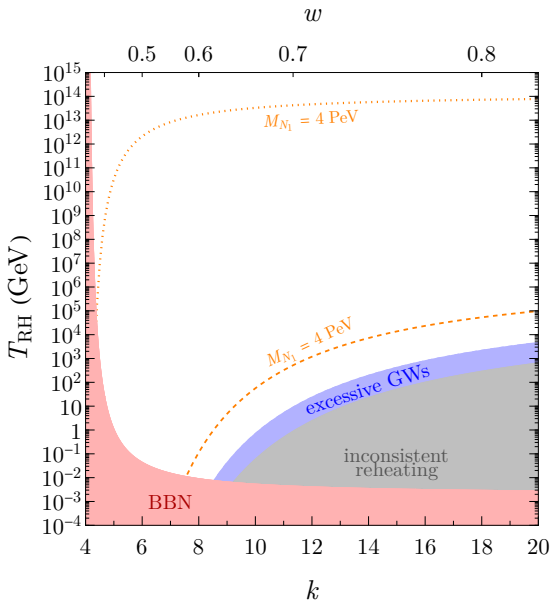

Figure 7. Contours of fixed relic density, $\Omega_{N_1}h^2 = 0.12$ for $M_{N_1} = 4\,\text{PeV}$. The upper dotted contour corresponds to production from gravitational scattering in the thermal bath (and requires a large value of ξ_h) and the lower dashed contour corresponds to production from inflaton scattering (and requires a relatively low value of ξ_h) Between the two contours $\Omega_{N_1}h^2 < 0.12$ for $M_{N_1} = 4$ PeV.

gravitational interactions is excluded by BBN for an excessive amount of gravitational waves as dark radiation. Thus we then need to go (slightly) beyond the minimal setup and include non-minimal gravitational interactions. We show in figure 7 contours for $\Omega_{N_1}h^2 = 0.12$ for $M_{N_1} = 4\,\text{PeV}$ in the (k, $T_{\rm RH}$) plane. The orange (dashed, dotted) lines correspond to the two dominant gravitational scattering processes involving the (inflaton, thermal particles) as discussed in the previous subsection. Note however that gravitational thermal production requires a high reheating temperature and is not compatible with the observed baryon asymmetry as can be understood from figure 5. In contrast, at lower $T_{\rm RH}$, the correct relic density can be produced from inflaton scattering with a lower value of $\xi_h \approx 2.5$. In the left panel of figure 6, we show, by the black vertical line segment, the range in M_{N_2} obtained from varying k while fixing $M_{N_1} = 4$ PeV. Note that, since N_1 is a long-lived stable relic, it does not contribute to the generation of the baryon asymmetry as its decay takes place below the electroweak phase transition. In addition, because the Yukawa coupling of N_1 is extremely small, its interactions which violate lepton number will not be in equilibrium, and hence will not wash out any of the asymmetry produced by N_2. We summarize our analysis in the tables presented in the conclusion.

5 Dark matter & leptogenesis with a Majoron

We have seen in the previous section that our result was particularly constrained because of the strong dependence of the production of the RHN on its mass M_{N_i}, limiting our allowed region to masses above a PeV. In this section, we consider an alternative mechanism. We

JHEP12(2022)072

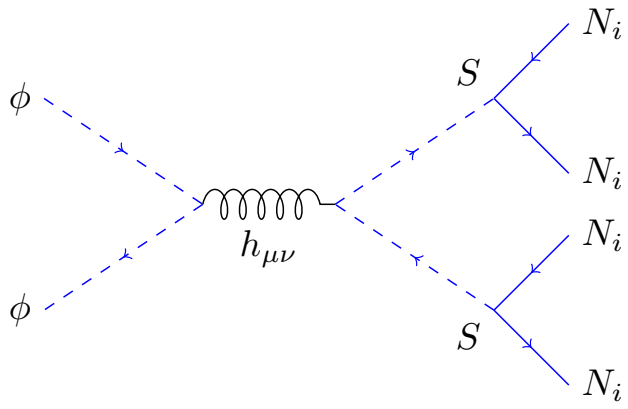

Figure 8. Feynman diagram for the gravitational production of an on-shell scalar S coupled to the heavy neutrinos.

include an additional complex scalar field, Φ containing the Majoron [99, 145, 156–163], that acts as an intermediate state in the interactions of the inflaton and RHNs. This interaction is depicted in figure 8.

The relevant Lagrangian of this extension can be written as

$$\mathcal{L}_\Phi = (-y_R^i \, \Phi \, \overline{N_i^c} \, N_i + \text{h.c.}) + \frac{1}{2}\mu_\Phi^2 \, \Phi^2 - \frac{1}{4}\lambda_\Phi \, \Phi^4 \, . \tag{5.1}$$

After symmetry breaking, the real part of Φ acquires a non-zero vacuum expectation value, around which one can expand the field as: $\Phi = \frac{1}{\sqrt{2}}(S + v_S)e^{iJ/v_S}$, and J is the Majoron. This expectation value is the origin of the RHN Majorana masses, $M_{N_i} = y_R^i \, v_S/\sqrt{2}$. Then $m_S = \mu_\Phi < m_\phi$ and the gravitational production rate of the real scalar, S is[10]

$$R_S^{\phi^k} = \frac{2 \times \rho_\phi^2}{16\pi M_P^4} \Sigma_S^k \, , \tag{5.2}$$

where the factor of two accounts for the fact we produce two scalar particles per scattering, with [65, 68]

$$\Sigma_S^k = \sum_{n=1}^{\infty} |\mathcal{P}_{2n}^k|^2 \left[1 + \frac{2\mu_\Phi^2}{E_{2n}^2}\right]^2 \sqrt{1 - \frac{4\mu_\Phi^2}{E_{2n}^2}} \, . \tag{5.3}$$

Since each scalar decays into 2 right-handed neutrinos, we obtain for the density of N_i after integration of the Boltzmann equation [68],

$$n_{N_i}^{S\phi^k}(a_{\rm RH}) \simeq \text{Br}_i \times \frac{\sqrt{3}\rho_{\rm RH}^{3/2}}{4\pi M_P^3} \frac{k+2}{6k-6} \left(\frac{\rho_{\rm end}}{\rho_{\rm RH}}\right)^{1-\frac{1}{k}} \Sigma_S^k, \tag{5.4}$$

[10] As shown in refs. [67, 68], for the case of a scalar field, the gravitational thermal production is always negligible with respect to inflaton scattering.

JHEP12(2022)072

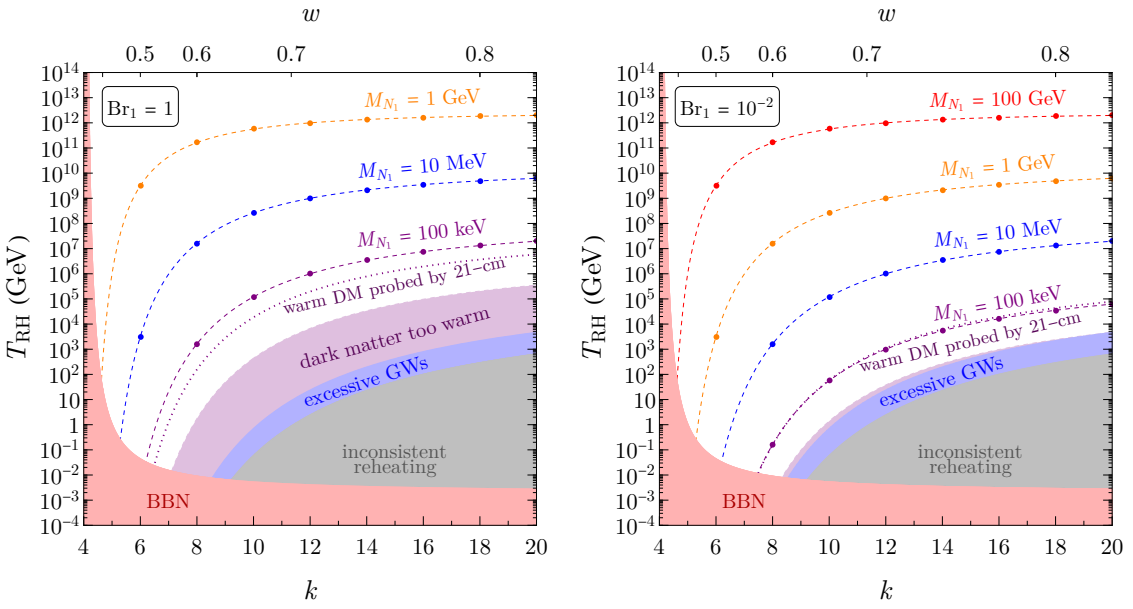

Figure 9. Contours of observed relic abundance assuming $\mathrm{Br}_1 = 1$ (left) and $\mathrm{Br}_1 = 10^{-2}$ (right) for different choices of the DM mass, considering only Majoron contribution. The purple-shaded region is disallowed from the warm DM limit (see text).

where we assumed $a_{\rm RH} \gg a_{\rm end}$, and here $\mathrm{Br}_i = \frac{(y_R^i)^2}{\sum (y_R^i)^2}$ so $\mathrm{Br}_i = \frac{M_{N_i}^2}{M_{N_1}^2+M_{N_2}^2+M_{N_3}^2}$ if $N_{1,2,3}$ are all lighter than S. The relic abundance of N_1 is then given by

$$\frac{\Omega_{N_1}^{S\phi^k} h^2}{0.12} \simeq \mathrm{Br}_1 \times \left(\frac{\rho_{\rm end}}{10^{64}\mathrm{GeV}^4}\right)^{1-\frac{1}{k}} \left(\frac{10^{40}\mathrm{GeV}^4}{\rho_{\rm RH}}\right)^{\frac{1}{4}-\frac{1}{k}} \left(\frac{k+2}{6k-6}\right) \times \Sigma_S^k \times \frac{M_{N_1}}{2.5\times 10^{\frac{24}{k}-8}\mathrm{GeV}}\,, \tag{5.5}$$

whereas the baryon asymmetry follows from eq. (3.24). Note that so long as $M_{N_i} \ll \mu_\Phi \ll m_\phi$, the resulting dark matter abundance and baryon asymmetry will be independent of m_S.

We show in figures 9 and 10 respectively, the parameter space allowed by the relic abundance and the baryogenesis constraint in the $(k\,, T_{\rm RH})$ plane. Comparing figure 9 and the dashed lines (from the inflaton scattering) in the bottom right panel of figure 4, we notice that the mass of the dark matter respecting Planck constraint is much lower, if the branching fraction to N_1 is large. For $\mathrm{Br}_1 = 1$, the difference is about 8 orders of magnitude, and around 6 orders of magnitude for $\mathrm{Br}_1 = 10^{-2}$. The reason is easy to understand: the production rate through S is boosted in comparison with the direct production, by a factor

$$\frac{R_{N_1}^{S\phi^k}}{R_{N_1}^{\phi^k}} \simeq \mathrm{Br}_1 \frac{m_\phi^2}{M_{N_1}^2}\,. \tag{5.6}$$

For smaller branching fraction, the density of N_1 through this channel is suppressed and the effect is milder and proportional to Br_1, as one can see in figure 9 right panel.

JHEP12(2022)072

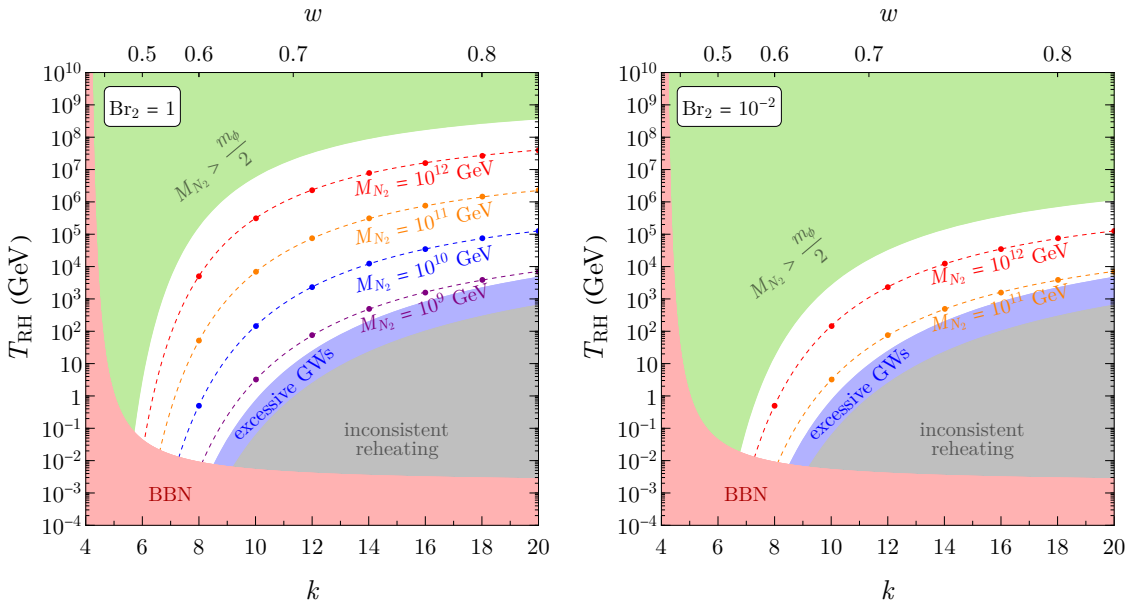

Figure 10. Contours of N_{N_2} corresponding to the observed baryon asymmetry for $\mathrm{Br}_2 = 1$ (left) and $\mathrm{Br}_2 = 10^{-2}$ (right) in the $(k, T_{\rm RH})$ plane. Here only the contribution due to the intermediate scalar is included. The green-shaded region is kinematically inaccessible due to $M_{N_2} > m_\phi/2$ [cf. figure 8].

Given that the required mass, M_{N_1}, can be much lower when we couple the RHNs to the scalar S, and N_1 is produced relativistically, N_1 dark matter may still be warm around the time of CMB decoupling. We derive the warmness constraint by redshifting the N_1 initial momentum of order m_ϕ at $T_{\rm max}$ to the temperature $T \simeq 1\,\mathrm{eV}$ and require that the velocity at $T \simeq 1\,\mathrm{eV}$ is less than 2×10^{-4}. This bound on the velocity is obtained from translating the limit on the warm dark matter mass from the Lyman-α forest [164] in the case where the abundance is generated thermally. The current warmness constraint is shown by the purple region, while the future sensitivity using cosmic 21-cm lines [165] is shown by the purple dotted curve. In summary, this mechanism interestingly allows for electroweak scale fermionic dark matter produced gravitationally, which is not possible by the direct scattering of the inflaton. We show in figure 10 the parameter space allowed to obtain a sufficient amount of baryon asymmetry for the set of branching ratios $\mathrm{Br}_2 = 1$ and 10^{-2}. Comparing figures 5 and 10 left, we note that for $M_2 = 10^{13}\,\mathrm{GeV}$ the situation is similar to the direct production because no real enhancement $\propto \frac{m_\phi^2}{M_{N_2}^2}$ exists. However, for $M_{N_2} = 10^{11}\,\mathrm{GeV}$ and large values of k, $T_{\rm RH}$ should be about 3 orders of magnitude larger to obtain the same asymmetry. The reason is that for a large value of k, $Y_B \propto \frac{1}{T_{\rm RH}}$ when S is produced (combining eqs. (5.4) and (3.24)), and $\propto \frac{M_{N_2}^2}{m_\phi^2 T_{\rm RH}}$ when N_2 is produced directly. In other words, $T_{\rm RH}$ should be compensated by a factor $\frac{m_\phi^2}{M_{N_2}^2}$ to avoid an excessive asymmetry. As in the case of dark matter, lowering the branching ratio dilutes the effect as one can see in the right panel of figure 10.

JHEP12(2022)072

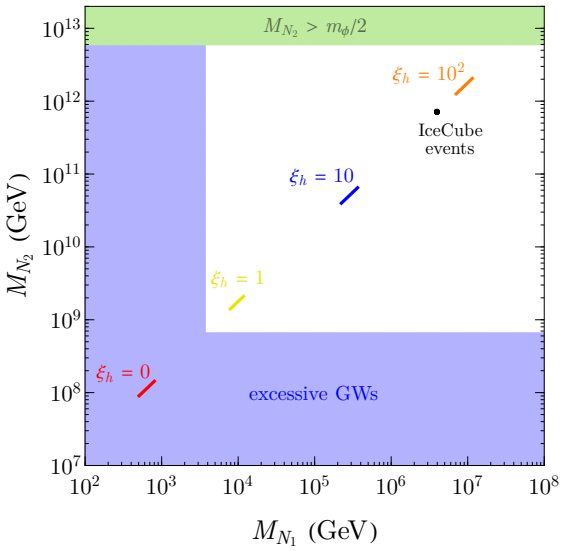

Figure 11. Parameter space satisfying the right dark matter relic abundance and baryon asymmetry, considering the production through S. The line colors correspond to different values of ξ_h, with $\xi_h = \{0, 1, 10, 10^2\}$ from bottom to top, and $\xi_h = 0$ corresponds to minimal graviton exchange. Each colored line segment shows the variation of the predicted masses with $k \in [6, 20]$. The black dot marks the parameter point that can also explain the IceCube high-energy neutrino excess.

Finally, we can combine all of the preceding results, adding the possibility for a gravitational reheating with non-minimal coupling. We illustrate this in figure 11, which is the analogue of figure 6 but with the scalar S as an intermediate state. For demonstration purposes, here we suppose $M_{N_3} > m_\phi/2$ so that N_3 is not produced by the inflaton or S, resulting in $\mathrm{Br}_2 = 1 - \mathrm{Br}_1 = 1 - (M_{N_1}/M_{N_2})^2 \simeq 1$. As the branching ratios are completely determined by the masses M_{N_1} and M_{N_2}, for a fixed k and a fixed ξ_h, there will be again only one point in the (M_{N_1}, M_{N_2}) plane that could simultaneously obtain the CMB-determined DM relic abundance and the observed baryon asymmetry. Each color segment in figure 11 assumes a fixed ξ_h and allows values of $k \in [6, 20]$ that are consistent with the BBN bound on T_{RH}. The black dot indicates the $M_{N_{1,2}}$ masses, independent of k, required to explain the IceCube high-energy neutrino excess. The green region is inaccessible because $m_S > M_{N_2} > m_\phi/2$ forbids the production of S via ϕ scattering.[11] Compared to figure 6, we see that the effect of S as an intermediate state expands the parameter space of allowed dark matter density and baryon asymmetry. Most notably, the parameter space opens up towards lower masses, and allows large values of ξ_h.

[11]Note that we have not included the effects of μ_Φ in Σ_S^k. These start to play a role for large $\xi_h \gtrsim 10^2$ when $2M_{N_2}$ becomes close to m_ϕ, since we require $2m_{N_2} < m_S < m_\phi$.

JHEP12(2022)072

Direct gravitational production			
ξ_h	$T_{\rm RH}$ [GeV]	M_{N_1} [PeV]	M_{N_2} [GeV]
1	$\{5.6\text{–}1.8 \times 10^4\}$	$\{2.49\text{–}2.54\}$	$\{4.5\text{–}4.8\} \times 10^{11}$
$\{2.5\text{–}2.7\}$	$\{0.11\text{–}9.8 \times 10^4\}$	$4.0\star$	$\{7.3\text{–}9.2\} \times 10^{11}$
10	8.1	8.1	1.7×10^{12}
Gravitational production via S			
ξ_h	$T_{\rm RH}$ [GeV]	M_{N_1}	M_{N_2} [GeV]
1	$\{5.6\text{–}1.8 \times 10^4\}$	$\{7.9\text{–}12\}$ TeV	$\{1.4\text{–}2.1\} \times 10^9$
10	$\{8.1\text{–}1.3 \times 10^6\}$	$\{220\text{–}360\}$ TeV	$\{4.0\text{–}6.5\} \times 10^{10}$
$\{50\text{–}68\}$	$\{2.6 \times 10^3\text{–}2.6 \times 10^7\}$	$4.0\,\text{PeV}\star$	7.1×10^{11}
100	$\{8.1 \times 10^3\text{–}9.8 \times 10^7\}$	$\{7.1\text{–}11\}$ PeV	$\{1.3\text{–}2.0\} \times 10^{12}$

Table 2. Ranges of $T_{\rm RH}$, DM (M_{N_1}) and RHN (M_{N_2}) masses, over which baryon asymmetry and DM relic abundance are simultaneously satisfied via gravitational yield for different choices of the non-minimal coupling ξ_h; $\xi_h = 0$ corresponds to minimal gravity, which is not shown since it is excluded by BBN for excessive GWs. The upper section assumes direction production of $N_{1,2}$, while the lower assumes production via Majoron's CP-even partner S as an intermediate state. Here we allow $k \in [6, 20]$ and omit points whose low $T_{\rm RH}$ values are excluded by BBN. (For the direct gravitational production, a single value of $k = 8$ is allowed for $\xi_h = 10$, while no points are allowed for $\xi_h \gtrsim 13.5$.) The $\star$ entry corresponds to the DM mass that can explain the IceCube high-energy neutrino events.

6 Conclusions

In this paper, we have shown that there exists the possibility that inflationary reheating, dark matter and the baryon asymmetry can be generated solely gravitational interactions. The baryon asymmetry is produced through the decay of a right-handed neutrino M_{N_2} (leading first to a non-zero lepton asymmetry). For minimal gravitational interactions, $\xi_h = 0$, a large amount of dark radiation is created in the form of gravitational waves and is inconsistent with BBN. Thus, we allow for a non-minimal gravitational coupling $\xi_h RH^2$ where H the Standard Model Higgs field to enhance reheating, so that the ratio of gravitational wave energy density to the radiation is decreased. The lowest ξ_h consistent with BBN is around 0.5. The range of the parameter space is 2–8 PeV for the dark matter mass M_{N_1} and $0.3\text{–}1.7 \times 10^{12}$ GeV for the mass of the lepton number violating decaying RHN, M_{N_2}. The range corresponds to a scan over ξ_h. Our solution restricts $0.5 \lesssim \xi_h \lesssim 13.5$ and $T_{\rm RH} < 3 \times 10^5$ GeV, where the maximum reheating temperature is attained with $\xi_h \simeq 4.7$. We summarize our results for fixing different values of ξ_h or M_{N_1} in the upper sections of table 2 and table 3 labeled "Direct gravitational production". Primordial gravitational waves generated during inflation allow a large parameter space with $T_{\rm RH} \lesssim 5 \times 10^6$ GeV to be probed in proposed gravitational wave detectors such as BBO, DECIGO, CE and ET.

We also showed that N_1, if unstable, can explain the recent IceCube PeV events through its decay into SM neutrinos. In this case, if we want to accommodate simultaneously the

JHEP12(2022)072

Direct gravitational production			
ξ_h	$T_{\rm RH}$ [GeV]	M_{N_1} [PeV]	M_{N_2} [GeV]
1	0.0084 (excluded)	—	—
2.5	0.11	4.0⋆	7.3×10^{11}
10	8.1	8.1	1.7×10^{12}
Gravitational production via S			
ξ_h	$T_{\rm RH}$ [GeV]	M_{N_1}	M_{N_2} [GeV]
1	0.0084 (excluded)	—	—
10	8.1	220 TeV	4.0×10^{10}
68	2.6×10^3	4.0⋆	7.1×10^{11}
100	8.1×10^3	7.1 PeV	1.3×10^{12}

Table 3. Same as table 2 but for a fixed $k = 8$ as a benchmark.

correct DM relic abundance, the observed baryon asymmetry, gravitational reheating and the IceCube events, the value of ξ_h is fixed for a given k. We show this result in the second row of the upper section of each table where the assumed value of $m_{N_1} = 4\,\text{PeV}$ is marked by $\star$.

Finally, we proposed a new scenario where the RHN and the dark matter are produced through an intermediate scalar state S, the CP-even partner of the Majoron. In this case, the gravitational production of the scalar is not helicity suppressed by the mass of the final state fermions. As a result, the mass ranges for N_1 and N_2 are increased. For $0.5 \lesssim \xi_h \lesssim 100$, the mass range for N_1 is 4 TeV to 11 PeV, and the range for N_2 is 7×10^8–2×10^{12} GeV. Finally, the IceCube events can be explained by appropriate choices of ξ_h and $T_{\rm RH}$ for each k, whereas M_{N_2} is predicted to be 7.1×10^{11} GeV for all k when M_{N_1} is fixed to 4 PeV. We summarize our overall results for fixing different values of ξ_h or M_{N_1} in the lower sections of table 2 and table 3 labeled "Gravitational production via S".

Acknowledgments

We would like to thank Essodjolo Kpatcha and Jong-Hyun Yoon for useful discussions. We thank Pedro Schwaller for bringing to our attention the constraint from the gravitational wave as dark radiation. BB received funding from the Patrimonio Autónomo — Fondo Nacional de Financiamiento para la Ciencia, la Tecnología y la Innovación Francisco José de Caldas (MinCiencias — Colombia) grant 80740-465-2020. This project has received funding /support from the European Union's Horizon 2020 research and innovation programme under the Marie Sklodowska-Curie grant agreement No 860881-HIDDeN, and the IN2P3 Master Projet UCMN. BB would also like to acknowledge the hospitality at the IJCLab during INVISIBLES'22 school+workshop, during which this work was initiated and fruitful discussions with Ashmita Das. The work of R.C. and K.A.O. was supported in part by DOE grant DE-SC0011842 at the University of Minnesota.

JHEP12(2022)072

References

[1] H. Poincaré, *The Milky Way and the Theory of Gases*, *Popular Astronomy* **14** (1906) 475.

[2] F. Zwicky, *Die Rotverschiebung von extragalaktischen Nebeln*, *Gen. Rel. Grav.* **41** (2009) 207 [*Helv. Phys. Acta* **6** (1933) 110] [INSPIRE].

[3] PLANCK collaboration, *Planck 2018 results. VI. Cosmological parameters*, *Astron. Astrophys.* **641** (2020) A6 [*Erratum ibid.* **652** (2021) C4] [arXiv:1807.06209] [INSPIRE].

[4] J.E. Gunn, B.W. Lee, I. Lerche, D.N. Schramm and G. Steigman, *Some Astrophysical Consequences of the Existence of a Heavy Stable Neutral Lepton*, *Astrophys. J.* **223** (1978) 1015 [INSPIRE].

[5] P. Hut, *Limits on Masses and Number of Neutral Weakly Interacting Particles*, *Phys. Lett. B* **69** (1977) 85 [INSPIRE].

[6] B.W. Lee and S. Weinberg, *Cosmological Lower Bound on Heavy Neutrino Masses*, *Phys. Rev. Lett.* **39** (1977) 165 [INSPIRE].

[7] J.R. Ellis, J.S. Hagelin, D.V. Nanopoulos, K.A. Olive and M. Srednicki, *Supersymmetric Relics from the Big Bang*, *Nucl. Phys. B* **238** (1984) 453 [INSPIRE].

[8] V. Silveira and A. Zee, *Scalar phantoms*, *Phys. Lett. B* **161** (1985) 136 [INSPIRE].

[9] J. McDonald, *Gauge singlet scalars as cold dark matter*, *Phys. Rev. D* **50** (1994) 3637 [hep-ph/0702143] [INSPIRE].

[10] C.P. Burgess, M. Pospelov and T. ter Veldhuis, *The Minimal model of nonbaryonic dark matter: A Singlet scalar*, *Nucl. Phys. B* **619** (2001) 709 [hep-ph/0011335] [INSPIRE].

[11] H. Davoudiasl, R. Kitano, T. Li and H. Murayama, *The New minimal standard model*, *Phys. Lett. B* **609** (2005) 117 [hep-ph/0405097] [INSPIRE].

[12] J.M. Cline, K. Kainulainen, P. Scott and C. Weniger, *Update on scalar singlet dark matter*, *Phys. Rev. D* **88** (2013) 055025 [*Erratum ibid.* **92** (2015) 039906] [arXiv:1306.4710] [INSPIRE].

[13] H. Han and S. Zheng, *New Constraints on Higgs-portal Scalar Dark Matter*, *JHEP* **12** (2015) 044 [arXiv:1509.01765] [INSPIRE].

[14] A. Djouadi, O. Lebedev, Y. Mambrini and J. Quevillon, *Implications of LHC searches for Higgs-portal dark matter*, *Phys. Lett. B* **709** (2012) 65 [arXiv:1112.3299] [INSPIRE].

[15] O. Lebedev, H.M. Lee and Y. Mambrini, *Vector Higgs-portal dark matter and the invisible Higgs*, *Phys. Lett. B* **707** (2012) 570 [arXiv:1111.4482] [INSPIRE].

[16] Y. Mambrini, *Higgs searches and singlet scalar dark matter: Combined constraints from XENON 100 and the LHC*, *Phys. Rev. D* **84** (2011) 115017 [arXiv:1108.0671] [INSPIRE].

[17] A. Djouadi, A. Falkowski, Y. Mambrini and J. Quevillon, *Direct Detection of Higgs-Portal Dark Matter at the LHC*, *Eur. Phys. J. C* **73** (2013) 2455 [arXiv:1205.3169] [INSPIRE].

JHEP12(2022)072

[18] J.A. Casas, D.G. Cerdeño, J.M. Moreno and J. Quilis, *Reopening the Higgs portal for single scalar dark matter*, *JHEP* **05** (2017) 036 [arXiv:1701.08134] [INSPIRE].

[19] G. Arcadi, Y. Mambrini and F. Richard, *Z-portal dark matter*, *JCAP* **03** (2015) 018 [arXiv:1411.2985] [INSPIRE].

[20] M. Escudero, A. Berlin, D. Hooper and M.-X. Lin, *Toward (Finally!) Ruling Out Z and Higgs Mediated Dark Matter Models*, *JCAP* **12** (2016) 029 [arXiv:1609.09079] [INSPIRE].

[21] L. Roszkowski, E.M. Sessolo and S. Trojanowski, *WIMP dark matter candidates and searches — current status and future prospects*, *Rept. Prog. Phys.* **81** (2018) 066201 [arXiv:1707.06277] [INSPIRE].

[22] G. Arcadi et al., *The waning of the WIMP? A review of models, searches, and constraints*, *Eur. Phys. J. C* **78** (2018) 203 [arXiv:1703.07364] [INSPIRE].

[23] Y. Mambrini, *The Kinetic dark-mixing in the light of CoGENT and XENON100*, *JCAP* **09** (2010) 022 [arXiv:1006.3318] [INSPIRE].

[24] O. Lebedev and Y. Mambrini, *Axial dark matter: The case for an invisible Z'*, *Phys. Lett. B* **734** (2014) 350 [arXiv:1403.4837] [INSPIRE].

[25] A. Alves, A. Berlin, S. Profumo and F.S. Queiroz, *Dark Matter Complementarity and the Z' Portal*, *Phys. Rev. D* **92** (2015) 083004 [arXiv:1501.03490] [INSPIRE].

[26] A. Alves, G. Arcadi, Y. Mambrini, S. Profumo and F.S. Queiroz, *Augury of darkness: the low-mass dark Z' portal*, *JHEP* **04** (2017) 164 [arXiv:1612.07282] [INSPIRE].

[27] G. Arcadi, P. Ghosh, Y. Mambrini, M. Pierre and F.S. Queiroz, *Z' portal to Chern-Simons Dark Matter*, *JCAP* **11** (2017) 020 [arXiv:1706.04198] [INSPIRE].

[28] D.V. Nanopoulos, K.A. Olive and M. Srednicki, *After Primordial Inflation*, *Phys. Lett. B* **127** (1983) 30 [INSPIRE].

[29] M.Y. Khlopov and A.D. Linde, *Is It Easy to Save the Gravitino?*, *Phys. Lett. B* **138** (1984) 265 [INSPIRE].

[30] K.A. Olive, D.N. Schramm and M. Srednicki, *Gravitinos as the Cold Dark Matter in an $\Omega = 1$ Universe*, *Nucl. Phys. B* **255** (1985) 495 [INSPIRE].

[31] J. McDonald, *Thermally generated gauge singlet scalars as selfinteracting dark matter*, *Phys. Rev. Lett.* **88** (2002) 091304 [hep-ph/0106249] [INSPIRE].

[32] L.J. Hall, K. Jedamzik, J. March-Russell and S.M. West, *Freeze-In Production of FIMP Dark Matter*, *JHEP* **03** (2010) 080 [arXiv:0911.1120] [INSPIRE].

[33] Y. Mambrini, K.A. Olive, J. Quevillon and B. Zaldivar, *Gauge Coupling Unification and Nonequilibrium Thermal Dark Matter*, *Phys. Rev. Lett.* **110** (2013) 241306 [arXiv:1302.4438] [INSPIRE].

[34] N. Bernal, M. Heikinheimo, T. Tenkanen, K. Tuominen and V. Vaskonen, *The Dawn of FIMP Dark Matter: A Review of Models and Constraints*, *Int. J. Mod. Phys. A* **32** (2017) 1730023 [arXiv:1706.07442] [INSPIRE].

[35] F. Elahi, C. Kolda and J. Unwin, *UltraViolet Freeze-in*, *JHEP* **03** (2015) 048 [arXiv:1410.6157] [INSPIRE].

[36] Y. Mambrini, N. Nagata, K.A. Olive, J. Quevillon and J. Zheng, *Dark matter and gauge coupling unification in nonsupersymmetric* SO(10) *grand unified models*, *Phys. Rev. D* **91** (2015) 095010 [arXiv:1502.06929] [INSPIRE].

JHEP12(2022)072

[37] G. Bhattacharyya, M. Dutra, Y. Mambrini and M. Pierre, *Freezing-in dark matter through a heavy invisible Z'*, *Phys. Rev. D* **98** (2018) 035038 [arXiv:1806.00016] [INSPIRE].

[38] D. Chowdhury, E. Dudas, M. Dutra and Y. Mambrini, *Moduli Portal Dark Matter*, *Phys. Rev. D* **99** (2019) 095028 [arXiv:1811.01947] [INSPIRE].

[39] K. Benakli, Y. Chen, E. Dudas and Y. Mambrini, *Minimal model of gravitino dark matter*, *Phys. Rev. D* **95** (2017) 095002 [arXiv:1701.06574] [INSPIRE].

[40] E. Dudas, Y. Mambrini and K. Olive, *Case for an EeV Gravitino*, *Phys. Rev. Lett.* **119** (2017) 051801 [arXiv:1704.03008] [INSPIRE].

[41] E. Dudas, T. Gherghetta, Y. Mambrini and K.A. Olive, *Inflation and High-Scale Supersymmetry with an EeV Gravitino*, *Phys. Rev. D* **96** (2017) 115032 [arXiv:1710.07341] [INSPIRE].

[42] E. Dudas, T. Gherghetta, K. Kaneta, Y. Mambrini and K.A. Olive, *Gravitino decay in high scale supersymmetry with R -parity violation*, *Phys. Rev. D* **98** (2018) 015030 [arXiv:1805.07342] [INSPIRE].

[43] K. Kaneta, Y. Mambrini, K.A. Olive and S. Verner, *Inflation and Leptogenesis in High-Scale Supersymmetry*, *Phys. Rev. D* **101** (2020) 015002 [arXiv:1911.02463] [INSPIRE].

[44] N. Bernal, M. Dutra, Y. Mambrini, K. Olive, M. Peloso and M. Pierre, *Spin-2 Portal Dark Matter*, *Phys. Rev. D* **97** (2018) 115020 [arXiv:1803.01866] [INSPIRE].

[45] K. Kaneta, Y. Mambrini and K.A. Olive, *Radiative production of nonthermal dark matter*, *Phys. Rev. D* **99** (2019) 063508 [arXiv:1901.04449] [INSPIRE].

[46] L. Heurtier and F. Huang, *Inflaton portal to a highly decoupled EeV dark matter particle*, *Phys. Rev. D* **100** (2019) 043507 [arXiv:1905.05191] [INSPIRE].

[47] Y. Mambrini, K.A. Olive and J. Zheng, *Post-inflationary dark matter bremsstrahlung*, *JCAP* **10** (2022) 055 [arXiv:2208.05859] [INSPIRE].

[48] D.J.H. Chung, E.W. Kolb and A. Riotto, *Production of massive particles during reheating*, *Phys. Rev. D* **60** (1999) 063504 [hep-ph/9809453] [INSPIRE].

[49] G.F. Giudice, E.W. Kolb and A. Riotto, *Largest temperature of the radiation era and its cosmological implications*, *Phys. Rev. D* **64** (2001) 023508 [hep-ph/0005123] [INSPIRE].

[50] M.A.G. Garcia, Y. Mambrini, K.A. Olive and M. Peloso, *Enhancement of the Dark Matter Abundance Before Reheating: Applications to Gravitino Dark Matter*, *Phys. Rev. D* **96** (2017) 103510 [arXiv:1709.01549] [INSPIRE].

[51] M.A.G. Garcia, K. Kaneta, Y. Mambrini and K.A. Olive, *Reheating and Post-inflationary Production of Dark Matter*, *Phys. Rev. D* **101** (2020) 123507 [arXiv:2004.08404] [INSPIRE].

[52] M.A.G. Garcia, K. Kaneta, Y. Mambrini and K.A. Olive, *Inflaton Oscillations and Post-Inflationary Reheating*, *JCAP* **04** (2021) 012 [arXiv:2012.10756] [INSPIRE].

[53] B. Barman, N. Bernal, Y. Xu and O. Zapata, *Ultraviolet freeze-in with a time-dependent inflaton decay*, *JCAP* **07** (2022) 019 [arXiv:2202.12906] [INSPIRE].

[54] Y. Ema, R. Jinno, K. Mukaida and K. Nakayama, *Gravitational Effects on Inflaton Decay*, *JCAP* **05** (2015) 038 [arXiv:1502.02475] [INSPIRE].

[55] M. Garny, M. Sandora and M.S. Sloth, *Planckian Interacting Massive Particles as Dark Matter*, *Phys. Rev. Lett.* **116** (2016) 101302 [arXiv:1511.03278] [INSPIRE].

JHEP12(2022)072

[56] M. Garny, A. Palessandro, M. Sandora and M.S. Sloth, *Theory and Phenomenology of Planckian Interacting Massive Particles as Dark Matter*, *JCAP* **02** (2018) 027 [arXiv:1709.09688] [INSPIRE].

[57] Y. Tang and Y.-L. Wu, *Pure Gravitational Dark Matter, Its Mass and Signatures*, *Phys. Lett. B* **758** (2016) 402 [arXiv:1604.04701] [INSPIRE].

[58] Y. Tang and Y.-L. Wu, *On Thermal Gravitational Contribution to Particle Production and Dark Matter*, *Phys. Lett. B* **774** (2017) 676 [arXiv:1708.05138] [INSPIRE].

[59] Y. Ema, R. Jinno, K. Mukaida and K. Nakayama, *Gravitational particle production in oscillating backgrounds and its cosmological implications*, *Phys. Rev. D* **94** (2016) 063517 [arXiv:1604.08898] [INSPIRE].

[60] Y. Ema, K. Nakayama and Y. Tang, *Production of Purely Gravitational Dark Matter*, *JHEP* **09** (2018) 135 [arXiv:1804.07471] [INSPIRE].

[61] Y. Ema, K. Nakayama and Y. Tang, *Production of purely gravitational dark matter: the case of fermion and vector boson*, *JHEP* **07** (2019) 060 [arXiv:1903.10973] [INSPIRE].

[62] M. Chianese, B. Fu and S.F. King, *Impact of Higgs portal on gravity-mediated production of superheavy dark matter*, *JCAP* **06** (2020) 019 [arXiv:2003.07366] [INSPIRE].

[63] M. Chianese, B. Fu and S.F. King, *Interplay between neutrino and gravity portals for FIMP dark matter*, *JCAP* **01** (2021) 034 [arXiv:2009.01847] [INSPIRE].

[64] M. Redi, A. Tesi and H. Tillim, *Gravitational Production of a Conformal Dark Sector*, *JHEP* **05** (2021) 010 [arXiv:2011.10565] [INSPIRE].

[65] Y. Mambrini and K.A. Olive, *Gravitational Production of Dark Matter during Reheating*, *Phys. Rev. D* **103** (2021) 115009 [arXiv:2102.06214] [INSPIRE].

[66] B. Barman and N. Bernal, *Gravitational SIMPs*, *JCAP* **06** (2021) 011 [arXiv:2104.10699] [INSPIRE].

[67] M.R. Haque and D. Maity, *Gravitational dark matter: Free streaming and phase space distribution*, *Phys. Rev. D* **106** (2022) 023506 [arXiv:2112.14668] [INSPIRE].

[68] S. Clery, Y. Mambrini, K.A. Olive and S. Verner, *Gravitational portals in the early Universe*, *Phys. Rev. D* **105** (2022) 075005 [arXiv:2112.15214] [INSPIRE].

[69] S. Clery, Y. Mambrini, K.A. Olive, A. Shkerin and S. Verner, *Gravitational portals with nonminimal couplings*, *Phys. Rev. D* **105** (2022) 095042 [arXiv:2203.02004] [INSPIRE].

[70] A. Ahmed, B. Grzadkowski and A. Socha, *Higgs Boson-Induced Reheating and Dark Matter Production*, *Symmetry* **14** (2022) 306 [INSPIRE].

[71] A. Ahmed, B. Grzadkowski and A. Socha, *Higgs boson induced reheating and ultraviolet frozen-in dark matter*, arXiv:2207.11218 [INSPIRE].

[72] M. Fukugita and T. Yanagida, *Baryogenesis Without Grand Unification*, *Phys. Lett. B* **174** (1986) 45 [INSPIRE].

[73] V.A. Kuzmin, V.A. Rubakov and M.E. Shaposhnikov, *On the Anomalous Electroweak Baryon Number Nonconservation in the Early Universe*, *Phys. Lett. B* **155** (1985) 36 [INSPIRE].

[74] W. Buchmüller, P. Di Bari and M. Plümacher, *Cosmic microwave background, matter-antimatter asymmetry and neutrino masses*, *Nucl. Phys. B* **643** (2002) 367 [*Erratum ibid.* **793** (2008) 362] [hep-ph/0205349] [INSPIRE].

JHEP12(2022)072

[75] W. Buchmüller, P. Di Bari and M. Plümacher, *The Neutrino mass window for baryogenesis*, *Nucl. Phys. B* **665** (2003) 445 [hep-ph/0302092] [INSPIRE].

[76] P.H. Chankowski and K. Turzynski, *Limits on T(reh) for thermal leptogenesis with hierarchical neutrino masses*, *Phys. Lett. B* **570** (2003) 198 [hep-ph/0306059] [INSPIRE].

[77] G.F. Giudice, A. Notari, M. Raidal, A. Riotto and A. Strumia, *Towards a complete theory of thermal leptogenesis in the SM and MSSM*, *Nucl. Phys. B* **685** (2004) 89 [hep-ph/0310123] [INSPIRE].

[78] S. Davidson and A. Ibarra, *A Lower bound on the right-handed neutrino mass from leptogenesis*, *Phys. Lett. B* **535** (2002) 25 [hep-ph/0202239] [INSPIRE].

[79] G.F. Giudice, M. Peloso, A. Riotto and I. Tkachev, *Production of massive fermions at preheating and leptogenesis*, *JHEP* **08** (1999) 014 [hep-ph/9905242] [INSPIRE].

[80] T. Asaka, K. Hamaguchi, M. Kawasaki and T. Yanagida, *Leptogenesis in inflaton decay*, *Phys. Lett. B* **464** (1999) 12 [hep-ph/9906366] [INSPIRE].

[81] G. Lazarides and Q. Shafi, *Origin of matter in the inflationary cosmology*, *Phys. Lett. B* **258** (1991) 305 [INSPIRE].

[82] B.A. Campbell, S. Davidson and K.A. Olive, *Inflation, neutrino baryogenesis, and (S)neutrino induced baryogenesis*, *Nucl. Phys. B* **399** (1993) 111 [hep-ph/9302223] [INSPIRE].

[83] F. Hahn-Woernle and M. Plümacher, *Effects of reheating on leptogenesis*, *Nucl. Phys. B* **806** (2009) 68 [arXiv:0801.3972] [INSPIRE].

[84] R.T. Co, Y. Mambrini and K.A. Olive, *Inflationary gravitational leptogenesis*, *Phys. Rev. D* **106** (2022) 075006 [arXiv:2205.01689] [INSPIRE].

[85] N. Bernal and C.S. Fong, *Dark matter and leptogenesis from gravitational production*, *JCAP* **06** (2021) 028 [arXiv:2103.06896] [INSPIRE].

[86] M.R. Haque and D. Maity, *Gravitational Reheating*, arXiv:2201.02348 [INSPIRE].

[87] D.G. Figueroa and E.H. Tanin, *Inconsistency of an inflationary sector coupled only to Einstein gravity*, *JCAP* **10** (2019) 050 [arXiv:1811.04093] [INSPIRE].

[88] R. Kallosh and A. Linde, *Universality Class in Conformal Inflation*, *JCAP* **07** (2013) 002 [arXiv:1306.5220] [INSPIRE].

[89] S.Y. Choi, J.S. Shim and H.S. Song, *Factorization and polarization in linearized gravity*, *Phys. Rev. D* **51** (1995) 2751 [hep-th/9411092] [INSPIRE].

[90] B.R. Holstein, *Graviton Physics*, *Am. J. Phys.* **74** (2006) 1002 [gr-qc/0607045] [INSPIRE].

[91] J. Ellis, M.A.G. Garcia, D.V. Nanopoulos and K.A. Olive, *Calculations of Inflaton Decays and Reheating: with Applications to No-Scale Inflation Models*, *JCAP* **07** (2015) 050 [arXiv:1505.06986] [INSPIRE].

[92] PLANCK collaboration, *Planck 2018 results. X. Constraints on inflation*, *Astron. Astrophys.* **641** (2020) A10 [arXiv:1807.06211] [INSPIRE].

[93] J. Ellis, M.A.G. Garcia, D.V. Nanopoulos, K.A. Olive and S. Verner, *BICEP/Keck constraints on attractor models of inflation and reheating*, *Phys. Rev. D* **105** (2022) 043504 [arXiv:2112.04466] [INSPIRE].

[94] P. Minkowski, $\mu \to e\gamma$ *at a Rate of One Out of* 10^9 *Muon Decays?*, *Phys. Lett. B* **67** (1977) 421 [INSPIRE].

JHEP12(2022)072

[95] M. Gell-Mann, P. Ramond and R. Slansky, *Complex Spinors and Unified Theories*, *Conf. Proc. C* **790927** (1979) 315 [arXiv:1306.4669] [INSPIRE].

[96] T. Yanagida, *Horizontal gauge symmetry and masses of neutrinos*, *Conf. Proc. C* **7902131** (1979) 95 [INSPIRE].

[97] R.N. Mohapatra and G. Senjanović, *Neutrino Mass and Spontaneous Parity Nonconservation*, *Phys. Rev. Lett.* **44** (1980) 912 [INSPIRE].

[98] J. Schechter and J.W.F. Valle, *Neutrino Masses in* SU(2) × U(1) *Theories*, *Phys. Rev. D* **22** (1980) 2227 [INSPIRE].

[99] J. Schechter and J.W.F. Valle, *Neutrino Decay and Spontaneous Violation of Lepton Number*, *Phys. Rev. D* **25** (1982) 774 [INSPIRE].

[100] P.H. Frampton, S.L. Glashow and T. Yanagida, *Cosmological sign of neutrino CP-violation*, *Phys. Lett. B* **548** (2002) 119 [hep-ph/0208157] [INSPIRE].

[101] M. Raidal and A. Strumia, *Predictions of the most minimal seesaw model*, *Phys. Lett. B* **553** (2003) 72 [hep-ph/0210021] [INSPIRE].

[102] A. Ibarra and G.G. Ross, *Neutrino phenomenology: The Case of two right-handed neutrinos*, *Phys. Lett. B* **591** (2004) 285 [hep-ph/0312138] [INSPIRE].

[103] T. Rink, *Leptonic CP violation in the minimal type-I seesaw model: Bottom-up phenomenology & top-down model building*, Master's Thesis, Ruprecht-Karls-Universität Heidelberg, Heidelberg, Germany (2017) [INSPIRE].

[104] K. Ichikawa, T. Suyama, T. Takahashi and M. Yamaguchi, *Primordial Curvature Fluctuation and Its Non-Gaussianity in Models with Modulated Reheating*, *Phys. Rev. D* **78** (2008) 063545 [arXiv:0807.3988] [INSPIRE].

[105] K. Kainulainen, S. Nurmi, T. Tenkanen, K. Tuominen and V. Vaskonen, *Isocurvature Constraints on Portal Couplings*, *JCAP* **06** (2016) 022 [arXiv:1601.07733] [INSPIRE].

[106] Y. Mambrini, *Particles in the dark Universe*, Springer (2021) [doi:10.1007/978-3-030-78139-2].

[107] K.D. Lozanov and M.A. Amin, *Equation of State and Duration to Radiation Domination after Inflation*, *Phys. Rev. Lett.* **119** (2017) 061301 [arXiv:1608.01213] [INSPIRE].

[108] K.D. Lozanov and M.A. Amin, *Self-resonance after inflation: oscillons, transients and radiation domination*, *Phys. Rev. D* **97** (2018) 023533 [arXiv:1710.06851] [INSPIRE].

[109] D. Maity and P. Saha, *(P)reheating after minimal Plateau Inflation and constraints from CMB*, *JCAP* **07** (2019) 018 [arXiv:1811.11173] [INSPIRE].

[110] M.A. Luty, *Baryogenesis via leptogenesis*, *Phys. Rev. D* **45** (1992) 455 [INSPIRE].

[111] M. Flanz, E.A. Paschos and U. Sarkar, *Baryogenesis from a lepton asymmetric universe*, *Phys. Lett. B* **345** (1995) 248 [*Erratum ibid.* **384** (1996) 487] [*Erratum ibid.* **382** (1996) 447] [hep-ph/9411366] [INSPIRE].

[112] L. Covi, E. Roulet and F. Vissani, *CP violating decays in leptogenesis scenarios*, *Phys. Lett. B* **384** (1996) 169 [hep-ph/9605319] [INSPIRE].

[113] W. Buchmüller, P. Di Bari and M. Plümacher, *Leptogenesis for pedestrians*, *Annals Phys.* **315** (2005) 305 [hep-ph/0401240] [INSPIRE].

[114] S. Davidson, E. Nardi and Y. Nir, *Leptogenesis*, *Phys. Rept.* **466** (2008) 105 [arXiv:0802.2962] [INSPIRE].

JHEP12(2022)072

[115] T. Asaka, H.B. Nielsen and Y. Takanishi, *Nonthermal leptogenesis from the heavier Majorana neutrinos*, *Nucl. Phys. B* **647** (2002) 252 [hep-ph/0207023] [INSPIRE].

[116] V.N. Senoguz and Q. Shafi, *GUT scale inflation, nonthermal leptogenesis, and atmospheric neutrino oscillations*, *Phys. Lett. B* **582** (2004) 6 [hep-ph/0309134] [INSPIRE].

[117] B. Barman, D. Borah and R. Roshan, *Nonthermal leptogenesis and UV freeze-in of dark matter: Impact of inflationary reheating*, *Phys. Rev. D* **104** (2021) 035022 [arXiv:2103.01675] [INSPIRE].

[118] T.-H. Yeh, J. Shelton, K.A. Olive and B.D. Fields, *Probing physics beyond the standard model: limits from BBN and the CMB independently and combined*, *JCAP* **10** (2022) 046 [arXiv:2207.13133] [INSPIRE].

[119] R.T. Co et al., *Gravitational wave and CMB probes of axion kination*, *JHEP* **09** (2022) 116 [arXiv:2108.09299] [INSPIRE].

[120] K. Saikawa and S. Shirai, *Primordial gravitational waves, precisely: The role of thermodynamics in the Standard Model*, *JCAP* **05** (2018) 035 [arXiv:1803.01038] [INSPIRE].

[121] T. Opferkuch, P. Schwaller and B.A. Stefanek, *Ricci Reheating*, *JCAP* **07** (2019) 016 [arXiv:1905.06823] [INSPIRE].

[122] M. Giovannini, *Gravitational waves constraints on postinflationary phases stiffer than radiation*, *Phys. Rev. D* **58** (1998) 083504 [hep-ph/9806329] [INSPIRE].

[123] J. Crowder and N.J. Cornish, *Beyond LISA: Exploring future gravitational wave missions*, *Phys. Rev. D* **72** (2005) 083005 [gr-qc/0506015] [INSPIRE].

[124] V. Corbin and N.J. Cornish, *Detecting the cosmic gravitational wave background with the big bang observer*, *Class. Quant. Grav.* **23** (2006) 2435 [gr-qc/0512039] [INSPIRE].

[125] G.M. Harry, P. Fritschel, D.A. Shaddock, W. Folkner and E.S. Phinney, *Laser interferometry for the big bang observer*, *Class. Quant. Grav.* **23** (2006) 4887 [*Erratum ibid.* **23** (2006) 7361] [INSPIRE].

[126] N. Seto, S. Kawamura and T. Nakamura, *Possibility of direct measurement of the acceleration of the universe using 0.1-Hz band laser interferometer gravitational wave antenna in space*, *Phys. Rev. Lett.* **87** (2001) 221103 [astro-ph/0108011] [INSPIRE].

[127] S. Kawamura et al., *The Japanese space gravitational wave antenna DECIGO*, *Class. Quant. Grav.* **23** (2006) S125 [INSPIRE].

[128] K. Yagi and N. Seto, *Detector configuration of DECIGO/BBO and identification of cosmological neutron-star binaries*, *Phys. Rev. D* **83** (2011) 044011 [*Erratum ibid.* **95** (2017) 109901] [arXiv:1101.3940] [INSPIRE].

[129] LIGO Scientific collaboration, *Exploring the Sensitivity of Next Generation Gravitational Wave Detectors*, *Class. Quant. Grav.* **34** (2017) 044001 [arXiv:1607.08697] [INSPIRE].

[130] D. Reitze et al., *Cosmic Explorer: The U.S. Contribution to Gravitational-Wave Astronomy beyond LIGO*, *Bull. Am. Astron. Soc.* **51** (2019) 035 [arXiv:1907.04833] [INSPIRE].

[131] M. Punturo et al., *The Einstein Telescope: A third-generation gravitational wave observatory*, *Class. Quant. Grav.* **27** (2010) 194002 [INSPIRE].

[132] S. Hild et al., *Sensitivity Studies for Third-Generation Gravitational Wave Observatories*, *Class. Quant. Grav.* **28** (2011) 094013 [arXiv:1012.0908] [INSPIRE].

JHEP12(2022)072

[133] B. Sathyaprakash et al., *Scientific Objectives of Einstein Telescope*, *Class. Quant. Grav.* **29** (2012) 124013 [*Erratum ibid.* **30** (2013) 079501] [arXiv:1206.0331] [INSPIRE].

[134] M. Maggiore et al., *Science Case for the Einstein Telescope*, *JCAP* **03** (2020) 050 [arXiv:1912.02622] [INSPIRE].

[135] K. Schmitz, *New Sensitivity Curves for Gravitational-Wave Signals from Cosmological Phase Transitions*, *JHEP* **01** (2021) 097 [arXiv:2002.04615] [INSPIRE].

[136] ICECUBE collaboration, *First observation of PeV-energy neutrinos with IceCube*, *Phys. Rev. Lett.* **111** (2013) 021103 [arXiv:1304.5356] [INSPIRE].

[137] ICECUBE collaboration, *Evidence for High-Energy Extraterrestrial Neutrinos at the IceCube Detector*, *Science* **342** (2013) 1242856 [arXiv:1311.5238] [INSPIRE].

[138] ICECUBE collaboration, *Observation of High-Energy Astrophysical Neutrinos in Three Years of IceCube Data*, *Phys. Rev. Lett.* **113** (2014) 101101 [arXiv:1405.5303] [INSPIRE].

[139] Y. Bai, R. Lu and J. Salvado, *Geometric Compatibility of IceCube TeV-PeV Neutrino Excess and its Galactic Dark Matter Origin*, *JHEP* **01** (2016) 161 [arXiv:1311.5864] [INSPIRE].

[140] T. Higaki, R. Kitano and R. Sato, *Neutrinoful Universe*, *JHEP* **07** (2014) 044 [arXiv:1405.0013] [INSPIRE].

[141] A. Esmaili, S.K. Kang and P.D. Serpico, *IceCube events and decaying dark matter: hints and constraints*, *JCAP* **12** (2014) 054 [arXiv:1410.5979] [INSPIRE].

[142] A. Bhattacharya, M.H. Reno and I. Sarcevic, *Reconciling neutrino flux from heavy dark matter decay and recent events at IceCube*, *JHEP* **06** (2014) 110 [arXiv:1403.1862] [INSPIRE].

[143] J. Zavala, *Galactic PeV neutrinos from dark matter annihilation*, *Phys. Rev. D* **89** (2014) 123516 [arXiv:1404.2932] [INSPIRE].

[144] C. Rott, K. Kohri and S.C. Park, *Superheavy dark matter and IceCube neutrino signals: Bounds on decaying dark matter*, *Phys. Rev. D* **92** (2015) 023529 [arXiv:1408.4575] [INSPIRE].

[145] E. Dudas, Y. Mambrini and K.A. Olive, *Monochromatic neutrinos generated by dark matter and the seesaw mechanism*, *Phys. Rev. D* **91** (2015) 075001 [arXiv:1412.3459] [INSPIRE].

[146] K. Murase, R. Laha, S. Ando and M. Ahlers, *Testing the Dark Matter Scenario for PeV Neutrinos Observed in IceCube*, *Phys. Rev. Lett.* **115** (2015) 071301 [arXiv:1503.04663] [INSPIRE].

[147] L.A. Anchordoqui et al., *IceCube neutrinos, decaying dark matter, and the Hubble constant*, *Phys. Rev. D* **92** (2015) 061301 [*Erratum ibid.* **94** (2016) 069901] [arXiv:1506.08788] [INSPIRE].

[148] P. Ko and Y. Tang, *IceCube Events from Heavy DM decays through the Right-handed Neutrino Portal*, *Phys. Lett. B* **751** (2015) 81 [arXiv:1508.02500] [INSPIRE].

[149] S.B. Roland, B. Shakya and J.D. Wells, *PeV neutrinos and a 3.5 keV x-ray line from a PeV-scale supersymmetric neutrino sector*, *Phys. Rev. D* **92** (2015) 095018 [arXiv:1506.08195] [INSPIRE].

[150] M. Chianese and A. Merle, *A Consistent Theory of Decaying Dark Matter Connecting IceCube to the Sesame Street*, *JCAP* **04** (2017) 017 [arXiv:1607.05283] [INSPIRE].

JHEP12(2022)072

[151] M. Re Fiorentin, V. Niro and N. Fornengo, *A consistent model for leptogenesis, dark matter and the IceCube signal*, *JHEP* **11** (2016) 022 [arXiv:1606.04445] [INSPIRE].

[152] M.A.G. Garcia, Y. Mambrini, K.A. Olive and S. Verner, *Case for decaying spin-3/2 dark matter*, *Phys. Rev. D* **102** (2020) 083533 [arXiv:2006.03325] [INSPIRE].

[153] C.A. Argüelles et al., *Dark Matter decay to neutrinos*, arXiv:2210.01303 [INSPIRE].

[154] P. Jizba and G. Lambiase, *Tsallis cosmology and its applications in dark matter physics with focus on IceCube high-energy neutrino data*, arXiv:2206.12910 [INSPIRE].

[155] M. Ahmadvand, *Filtered asymmetric dark matter during the Peccei-Quinn phase transition*, *JHEP* **10** (2021) 109 [arXiv:2108.00958] [INSPIRE].

[156] Y. Chikashige, R.N. Mohapatra and R.D. Peccei, *Are There Real Goldstone Bosons Associated with Broken Lepton Number?*, *Phys. Lett. B* **98** (1981) 265 [INSPIRE].

[157] V. Berezinsky and J.W.F. Valle, *The KeV majoron as a dark matter particle*, *Phys. Lett. B* **318** (1993) 360 [hep-ph/9309214] [INSPIRE].

[158] M. Lattanzi and J.W.F. Valle, *Decaying warm dark matter and neutrino masses*, *Phys. Rev. Lett.* **99** (2007) 121301 [arXiv:0705.2406] [INSPIRE].

[159] F. Bazzocchi, M. Lattanzi, S. Riemer-Sørensen and J.W.F. Valle, *X-ray photons from late-decaying majoron dark matter*, *JCAP* **08** (2008) 013 [arXiv:0805.2372] [INSPIRE].

[160] M. Lattanzi, S. Riemer-Sorensen, M. Tortola and J.W.F. Valle, *Updated CMB and x- and γ-ray constraints on Majoron dark matter*, *Phys. Rev. D* **88** (2013) 063528 [arXiv:1303.4685] [INSPIRE].

[161] M. Lattanzi, R.A. Lineros and M. Taoso, *Connecting neutrino physics with dark matter*, *New J. Phys.* **16** (2014) 125012 [arXiv:1406.0004] [INSPIRE].

[162] J. Gehrlein and M. Pierre, *A testable hidden-sector model for Dark Matter and neutrino masses*, *JHEP* **02** (2020) 068 [arXiv:1912.06661] [INSPIRE].

[163] E. Dudas, L. Heurtier, Y. Mambrini, K.A. Olive and M. Pierre, *Model of metastable EeV dark matter*, *Phys. Rev. D* **101** (2020) 115029 [arXiv:2003.02846] [INSPIRE].

[164] V. Iršič et al., *New Constraints on the free-streaming of warm dark matter from intermediate and small scale Lyman-α forest data*, *Phys. Rev. D* **96** (2017) 023522 [arXiv:1702.01764] [INSPIRE].

[165] M. Sitwell, A. Mesinger, Y.-Z. Ma and K. Sigurdson, *The Imprint of Warm Dark Matter on the Cosmological 21-cm Signal*, *Mon. Not. Roy. Astron. Soc.* **438** (2014) 2664 [arXiv:1310.0029] [INSPIRE].

JHEP12(2022)072